ORKUSTOFNUN
NATIONAL ENERGY AUTHORITY
GEOTHERMAL DIVISION

Helga Tulinius
Amanda L. Spencer
Guðmundur S. Böðvarsson
Hrefna Kristmannsdóttir
Þorsteinn Thorsteinsson
Árný E. Sveinbjörnsdóttir

RESERVOIR STUDIES OF THE SELTJARNARNES GEOTHERMAL FIELD, ICELAND

OS-87032/JHD-07
Reykjavík, July 1987

ORKUSTOFNUN
NATIONAL ENERGY AUTHORITY
GEOTHERMAL DIVISION

GRENSÁSVEGUR 9,
108 REYKJAVÍK ICELAND

Helga Tulinius
Amanda L. Spencer
Guðmundur S. Böðvarsson
Hrefna Kristmannsdóttir
Þorsteinn Thorsteinsson
Árný E. Sveinbjörnsdóttir

RESERVOIR STUDIES OF THE SELTJARNARNES GEOTHERMAL FIELD, ICELAND

OS-87032/JHD-07
Reykjavík, July 1987

ABSTRACT

The Seltjarnarnes geothermal field in Iceland has been exploited for space heating for the last 16 years. A distributed parameter model of the field has been developed that integrates all available data. The model has been calibrated against the flow rate and pressure decline histories of the wells and the temperature and chemical changes of the produced fluids. This has allowed for the estimation of the permeability and porosity distribution of the system, and of the volume of the hot reservoir. The model used to match the data has six regions of different permeabilities and porosites. The well field lies within a region of high permeability (80 md) and low porosity (2%). The porosities increase away from the field up to 15% at a distance of 4 km. Predictions of future reservoir behavior using the model suggest small pressure and temperature changes. It indicates an average pressure drawdown of 15.5 bar over 20 years and a maximum temperature decline of 9°C, if the production of the field were to increase by 30 l/s every five years beginning in 1991. A continuous increase in the salinity of the fluids produced is, however, expected.

TABLE OF CONTENTS

		Page
ABSTRACT		2
1	INTRODUCTION	7
2	PREVIOUS WORK ON THE SELTJARNARNES FIELD	9
	2.1 Geology	9
	2.2 Aquifers	11
	2.3 Formation Temperature and Pressure	13
	2.4 Chemistry	16
	2.5 Well Testing	20
	2.6 Production	24
	2.7 Well Logging	27
3	CONCEPTUAL MODEL	28
4	NUMERICAL SIMULATIONS	30
	4.1 The Computer Programs	30
	4.2 Numerical Model	30
	4.3 Simulation Results	33
	4.4 Sensitivity Studies	35
	4.5 Chemistry and Temperature Match	35
5	PERFORMANCE PREDICTIONS	47
6	CONCLUSIONS	51
7	ACKNOWLEDGEMENTS	52
REFERENCES		53

LIST OF FIGURES

		Page
1.	Location Map of the Area	7
2.	Geological Cross-Section through Wells SN-01 to SN-06	10
3.	Locations of Aquifers	12
4.	Estimated Formation Temperature around Well SN-01	14
5.	Estimated Formation Temperature around Well SN-02	14
6.	Estimated Formation Temperature around Well SN-03	14
7.	Estimated Formation Temperature around Well SN-04	14
8.	Estimated Formation Temperature around Well SN-05	15
9.	Estimated Formation Temperature around Well SN-06	15
10.	Formation Temperature Profiles for Wells SN-01 to SN-06	15
11.	Changes in Total Dissolved Solids with Time in Wells in the Seltjarnarnes Field	17
12.	Changes in Chloride Concentration with Time in Wells in the Seltjarnarnes Field	17
13.	Changes in Silica Concentration with Time in Wells in the Seltjarnarnes Field	18
14.	Changes in δ^{18} with Time in Wells in the Seltjarnarnes Field	18
15.	Downhole Samples from 1966 to 1986 in Wells SN-01, SN-02, SN-03 and SN-04	19
16.	Changes in Water Level in Well SN-02 due to Production in Wells SN-03, SN-04 and SN-05 from 1973 to 1984.	21
17.	Calculated Short Term Drawdown in Wells SN-01, SN-03 - SN-06	23
18.	Interference Tests in Wells SN-01, SN-02 and SN-03 in 1970	24
19.	Production from Wells SN-02 to SN-05 from 1966 to 1984	25

Page

20. Production Times for the Wells 26

21. Cumulative Production 26

22. Conceptual Model of the Seltjarnarnes Area 29

23. The Mesh Used in the Simulation and the Permeability and Porosity Regions 32

24. Interference Tests, Data and Calculated Curves 34

25. Production History, Data and Calculated Curve 34

26. Simple Model of the Seltjarnarnes Geothermal Field 36

27. Plot of Silica versus Time Showing the Match between the simple Numerical Model and Field Data. Using the Simple Model 38

28. Plot of Chloride versus Time Showing the Match between the simple Numerical Model and Field Data. Using the Simple Model 38

29. Plot of Sodium versus Time Showing the Match between the simple Numerical Model and Field Data. Using the Simple Model 39

30. Plot of Oxygen-18 versus Time Showing the Match between the simple Numerical Model and Field Data. Using the Simple Model 39

31. Silica versus Time without Kinetic Transport Using the "Best" Simple Model 40

32. Chloride versus Time Showing the Match between the Numerical Model and Data for Individual Wells 43

33. Sodium versus Time Showing the Match between the Numerical Model and Data for Individual Wells 44

34. Silica versus Time Showing the Match between the Numerical Model and Data for Individual Wells 45

35. Oxygen-18 versus Time Showing the Match between the Numerical Model and Data for Individual Wells 46

36. Suggested Boundary between Seawater and Meteoric Water 48

37. Pressure Performance Predictions 49

LIST OF TABLES

		Page
1.	Production Characteristics of Wells in the Seltjarnarnes Geothermal Field	8
2.	Aquifers in Wells SN-03 - SN -06	12
3.	Well Tests in Wells SN-01 to SN-06	22
4.	Calculated Drawdown in Wells SN-01 and SN-03 - SN-06 from Well Tests	23
5.	Parameters Used in the Simulations	31
6.	Values for the Concentrations of the Chemical Species for the Different Fluids Used in Modeling the Seltjarnarnes Geothermal Field.	41

1 INTRODUCTION

The Seltjarnarnes geothermal area is located within the town Seltjarnarnes which is a suburb of Reykjavik, the capital city of Iceland (Figure 1). The field has been exploited for the past 16 years and provides hot water for the central heating of the Seltjarnarnes town.

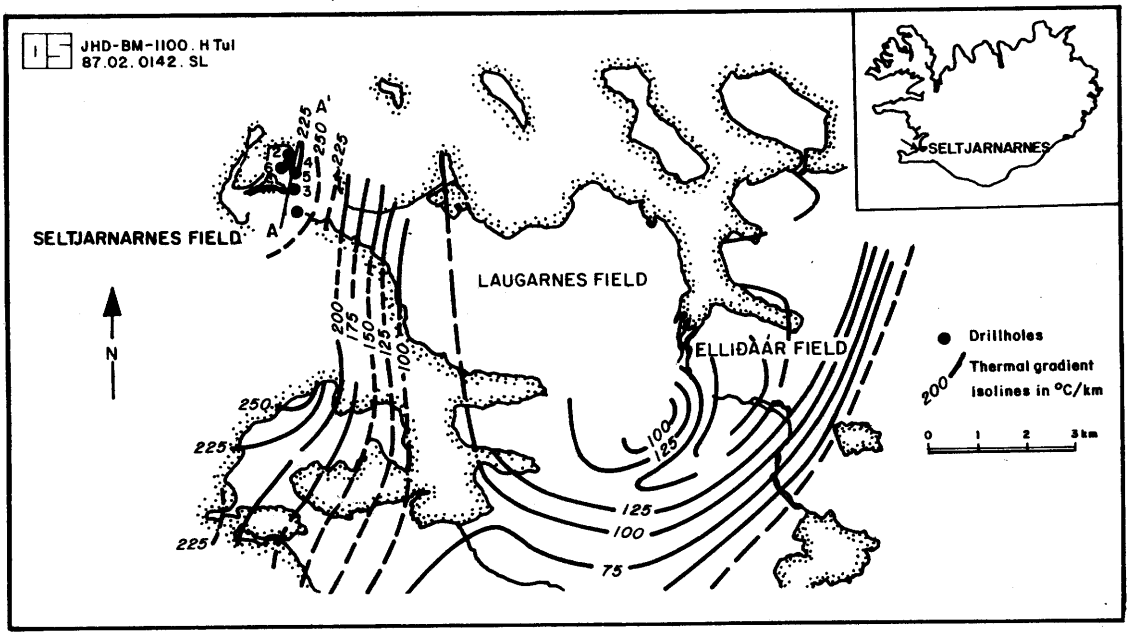

FIGURE 1 Location Map of the Area

The Seltjarnarnes field is a typical low temperature geothermal field with a temperature of about 100°C at 1000 m depth, and over 140°C at 2700m depth. The reservoir rocks are primarily 1.8-2.8 million years old Quaternary basaltic lavas and hyaloclastites (Jens Tómasson, et al, 1977). The geothermal water is of meteoric origin and has been traced by deuterium analyses to precipitation falling on the southernmost part of the glacier Langjökull, about 80 km to the NE (Bragi Árnason, 1976).

Several geothermal fields are located within or around Reykjavik (Figure 1). All of the geothermal fields are located within the same resistivity low (50 ohmm; Lúðvík Georgsson, 1985), and they all have high thermal gradient (> 150°C/km) in the uppermost 200 m (Helga Tulinius et al, 1986). The fields are separated by lower thermal gradients (< 100°C/km). Stable isotopes of fluids in the different geothermal fields in the area show that the fluids in the Seltjarnar-

nes reservoir have different origin from those produced in the Laugarnes and Ellidaár fields (Jens Tómasson et al., 1977; Bragi Árnason, 1976). These data and the lack of hydrological connections suggest that low permeability rocks (or impermeable faults) separate the Seltjarnarnes reservoir from the other systems (Þorsteinn Thorsteinsson and Jónas Elíasson, 1970).

Drilling in the Seltjarnarnes area started in 1965, with wells SN-01 and SN-02 being drilled to depths of 98 m and 80.7 m, respectively. These wells were originally drilled to estimate the thermal gradient in the area, but were later deepened; well SN-01 to 1282 m in 1967, and well SN-02 to 856 m in1965. The drilling continued in 1970 with a 1715 m deep well (SN-03) and in 1972 with a 2025 m deep well (SN-04).

After the deepening of well SN-01 it yielded about 1 l/s and later produced about 3 l/s for about one year. Well SN-02 discharged about 3 l/s from August 1966 to October 1971 or a total of 400 million liters. Flow from well SN-02 ceased soon after production from SN-03 started. Wells SN-01 and SN-02 are now used as observation wells.

After the completion of well SN-04 the Seltjarnarnes Municipial District Heating Service was founded, being supplied with water from SN-03 and SN-04; these wells were capable of 40 l/s production. The next well was drilled in 1981 to a depth of 2207 m (SN-05) and the last well, SN-06 was drilled in 1985 to a depth of 2701 m. Maximum yield of these four producing wells is now 110 l/s (see Table 1), which is sufficient for space heating of the entire town (population 3600).

TABLE 1 Production Characteristics of Wells in the Seltjarnarnes Geothermal Field

Well	Year drilled	Depth (m)	Casing (m)	Max yield (l/s)	Water temperature (°C)
SN-01	1967	1282	18.5		
SN-02	1965	856	81.5		
SN-03	1970	1715	99	15	101-103
SN-04	1972	2025	172	35	111-116
SN-05	1981	2207	168	30	90-100
SN-06	1985	2701	414	30	115-117
				110	

In the summer of 1986 all available data on the Seltjarnarnes field from the different disciplines (geology, geophysics, chemistry and reservoir engineering) were collected and integrated into a conceptual model for reservoir simulation studies. The main objective of this work was to simulate the production history and interference tests to calibrate the model to the field's behavior. This model was then used to predict changes in pressure, temperature and chemical composition with future production. The work was done at Lawrence Berkeley Laboratory in California, U.S.A.

2 PREVIOUS WORK ON THE SELTJARNARNES FIELD

Since the drilling of the first well in 1965 a considerable amount of data has been collected and several reports describing the field have been published. In 1977 an overview report on the characteristics of most of the geothermal areas within and around Reykjavik was published (Jens Tómasson, et al., 1977). At that time four wells had been drilled at Seltjarnarnes, and in the report data available at that time for these wells (geology, well logs, well tests, aquifers) were given, along with a general model of the field. Other general reports on the field have been published by Guðmundur Pálmason et al. (1983); Hrefna Kristmannsdóttir (1986); and Ómar Sigurðsson et al. (1985). More specific reports have also been written on drilling, fracturing and pressure testing before completion of individual wells, well logs, well tests, fluid chemistry and other aspects of the Seltjarnarnes field (Árný E. Sveinbjörnsdóttir et al., 1984a, b; Hrefna Kristmannsdóttir, 1983, 1984a, b, c; Hrefna Kristmannsdóttir and Helga Tulinius, 1984; Hrefna Kristmannsdóttir et al., 1984; Jens Tómasson and Kristján Sæmundsson, 1970; Svanbjörg H. Haraldsdóttir, 1984a, b, c; Þorsteinn Thorsteinsson, 1970a, b, 1980, 1985; Þorsteinn Thorsteinsson and Jens Tómasson, 1972; and Þorsteinn Thorsteinsson et al., 1985).

2.1 Geology

The geothermal field at Seltjarnarnes and the other fields within and around Reykjavik are situated within the Kjalarnes caldera (Jens Tómasson et al., 1977). Figure 2 shows a simplified geological cross-section of the Seltjarnarnes field, extending from well SN-01 in the south to well SN-02 in the north (line AA' on Figure 1). The geological profile is based on analyses of drill cuttings collected at 2 m intervals during drilling (Jens Tómasson et al., 1977; Árný E. Sveinbjörnsdóttir et al., 1984a, b and 1986). The reservoir rocks are

mainly 1.8-2.8 m.ys old Quaternary rocks, with a general dip to the southeast and strike in almost the same direction as that of cross-section AA' in Figure 1. As shown in Figure 2 the rocks have been divided into 7 main groups (8 for well SN-06) of Quaternary basaltic lavas and hyaloclastites with few small sedimentary layers and intrusions that increase in frequency with depth. The Figure also shows that the geological structure under the Seltjarnarnes area is nearly horizontal.

Some high-grade alteration minerals (epidote, chlorite) have been observed in the drill-cuttings, which demonstrate that the Seltjarnarnes field was hotter at some earlier time.

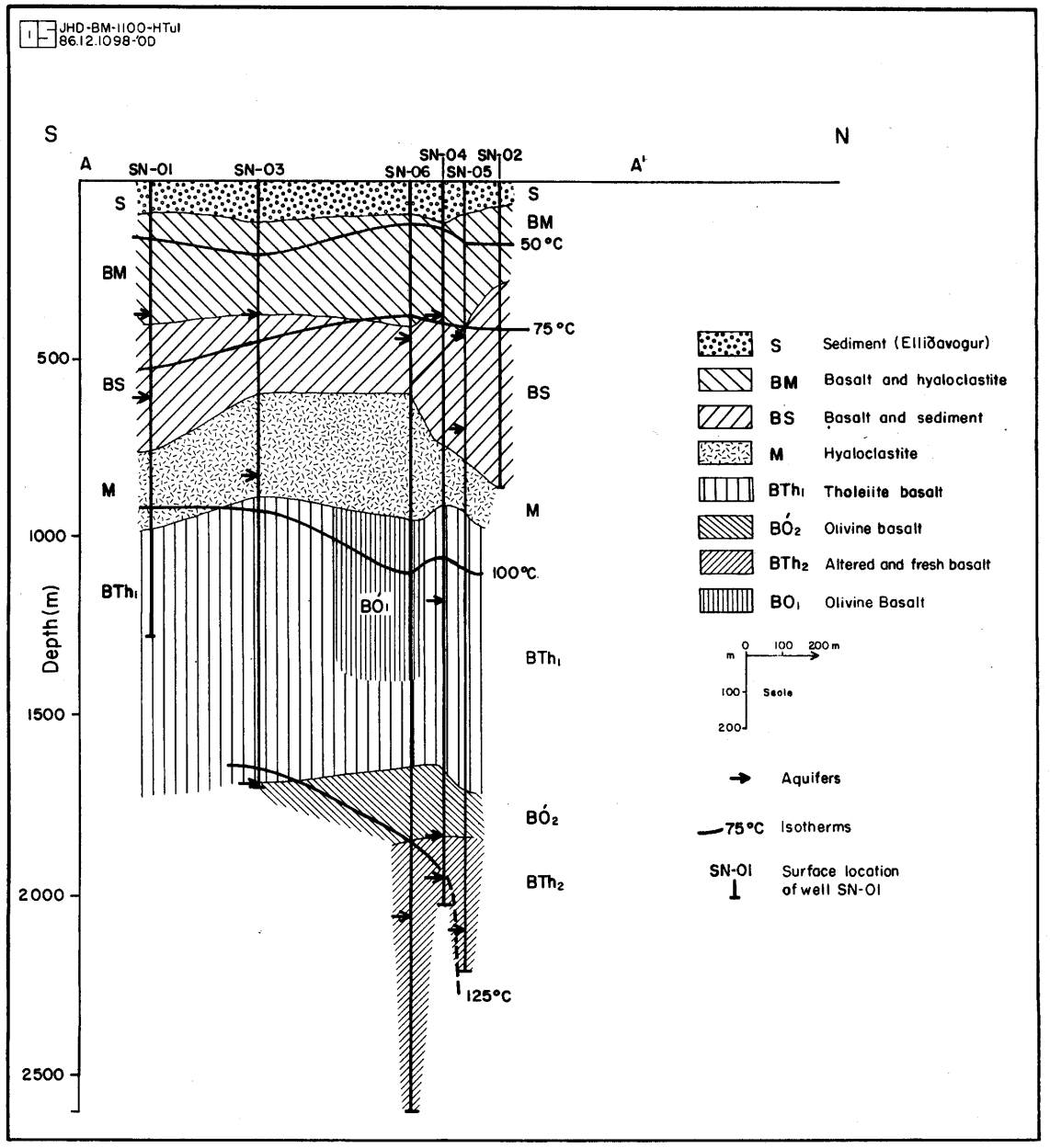

FIGURE 2 Geological Cross-section through Wells SN-01 to SN-06

2.2 Aquifers

Several aquifers have been detected in all of the wells (Jens Tómasson et al., 1977; Svanbjörg H. Haraldsdóttir, 1984a, b, c; Árný E. Sveinbjörnsdóttir et al., 1984a, b, 1986). The locations of the aquifers are based upon water losses (gains) during drilling or from temperature logs during the heating period. All known aquifers are shown in Figure 3 as arrows; and the main feedzones are shown on Figure 2. Table 2 gives the depth, estimated temperature, chloride concentration and rough estimate of percent production from each major aquifer for wells SN-03 - SN-06. All of the wells have at least three aquifers, and up to nine in well SN-06 (Figure 3).

About 1 l/s flowed from well SN-01 aftir it was deepened in 1967 and it produced about 3 l/s for space heating in 1969. Well SN-02 produced about 3 l/s from July 1966 to September 1971. The water temperature was about 78°C, and three aquifers, at 580 m-710 m depth, fed the well. Flow ceased from the well in 1971, and presently the well is used to monitor the water level changes due to production from wells SN-03 - SN-06.

All of the four production wells have an aquifer at around 400 m at the intersection between the BM and BS layers (Figure 2). There is also an indication that there is an aquifer at that depth in well SN-01, and it may be present in well SN-02 even though it does not show up in the temperature logs. This aquifer probably contains very saline water with an average temperature of 75°C - 80°C. The most productive aquifer in the field is located below 1700 m depth with a temperature of 125°C. In wells SN-03 and SN-05, 30% - 40% of the water comes from this aquifer, but up to 80% in wells SN-04 and SN-06. There are a few scattered aquifers between those two major ones, most of them above 900 m.

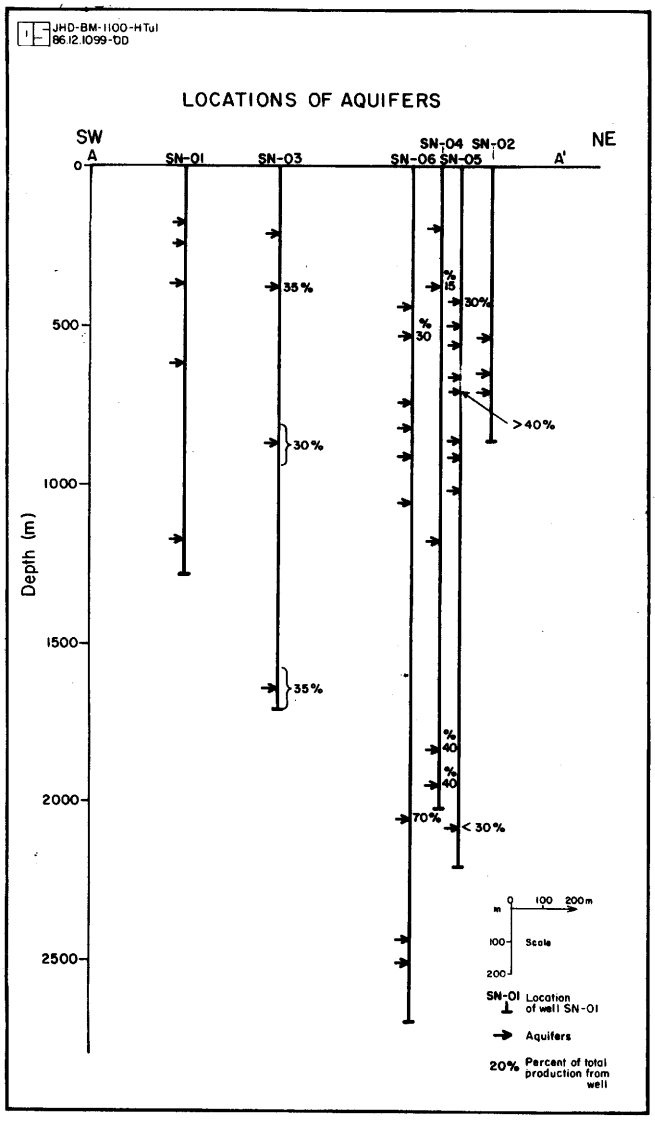

FIGURE 3 Locations of Aquifers

TABLE 2 Main Aquifers in Wells SN-03 - SN-06

Well	Depth (m)	Temperature (°C)	Cl concentration 1984 (ppm)	Production (%)
SN-03	380	72	2100	35
SN-03	870-930	100	1000	30
SN-03	1700	127	1000	35
SN-04	370	75	2000	15
SN-04	1180	104	900	5
SN-04	1840	122	900	40
SN-04	1950	126	900	40
SN-05	430	75	1800	30
SN-05	700	90	800	>40
SN-05	2090	>120	800	<30
SN-06	440-700	80	2100	30
SN-06	2060	133	1000	70

2.3 Formation Temperature and Pressure

Several downhole temperature surveys have been conducted for each of the wells (Jens Tómasson et al., 1977; Svanbjörg H. Haraldsdóttir, 1984a, b, c; Árný E. Sveinbjörnsdóttir et al., 1984a, b). In most cases the temperature profiles do not show the correct static formation temperature, as the wells have not reached equilibrium with the surrounding rock after drilling or production, or there is internal flow between aquifers in the wells.

Figures 4 through 9 show the estimated formation temperature for each of the six wells, but Figure 10 shows the estimated formation temperature profiles for all of the wells. One can see that they look very similar. The temperature increases rapidly with depth down to 200 m - 400 m where the slope decreases. At 400 m depth the temperature is 75°C - 80°C and at 1000 m it is around 100°C. All of the profiles show an increase in temperature with depth down to the bottom of the wells, with about 300°C/km gradient in the uppermost 200 m and about 35°C/km below 600 m depth. The highest temperature (>140°C) is in well SN-06 at 2700 m depth. The average temperature for the interval 400 m - 2200 m, where most of the aquifers are located, is about 110°C.

Isotherms along the cross-section AA` are plotted in Figure 2. The temperature appears to be fairly uniform over the entire wellfield especially above 1500 m. Below that depth the temperatures are higher in the southern part, and well SN-05 is somewhat colder than the other wells below 2000 m depth. This could either indicate that hot water recharges the reservoir from the southeast or that colder waters are present close to well SN-05. An attempt was made to plot contour map of isotherms for several depths, but since the well locations fall approximately on a straight line no additional information was gained on the subsurface temperature distribution.

Not much is known of the initial reservoir pressure, but after well SN-02 was deepened in 1967 it had a wellhead pressure of several meters. In 1970 the shut-in wellhead pressure was 13 m a.s.l. Well SN-04 had a shut-in wellhead pressure of 30 bar in July 1972 shortly before it started producing. The pressure changes in the area due to production have been monitored since May 1973 using water level changes in well SN-02.

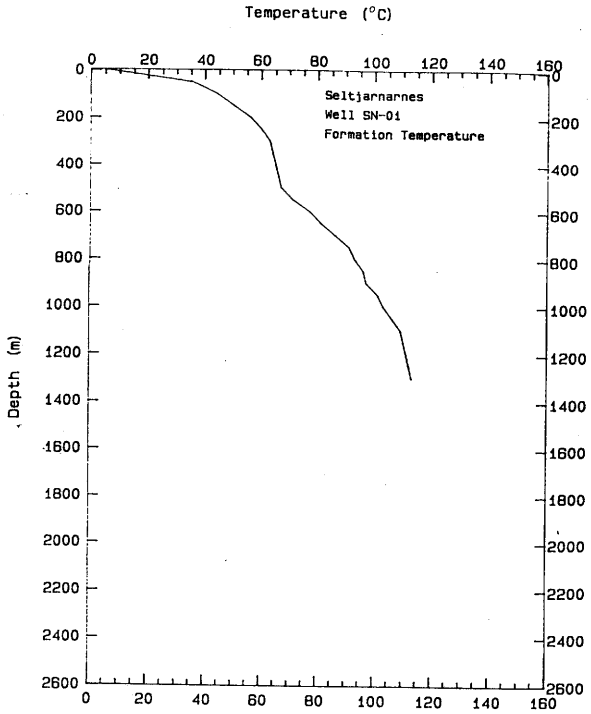

FIGURE 4 Estimated Formation Temperature around Well SN-01

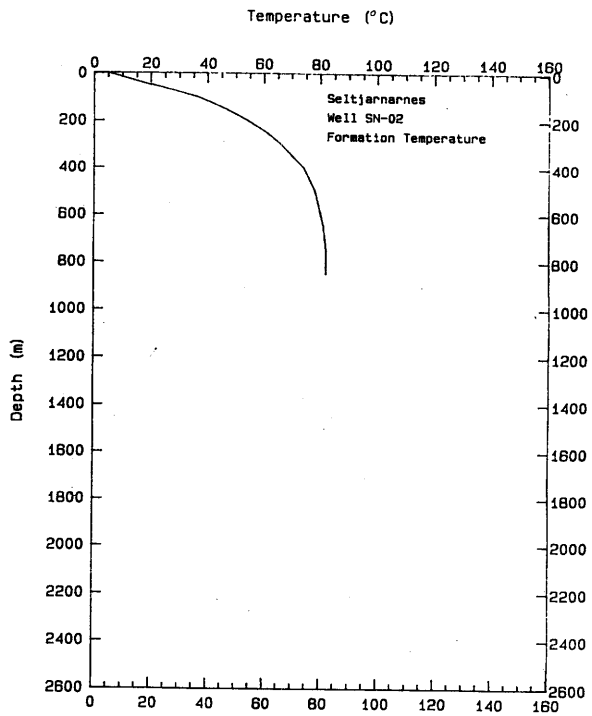

FIGURE 5 Estimated Formation Temperature around Well SN-02

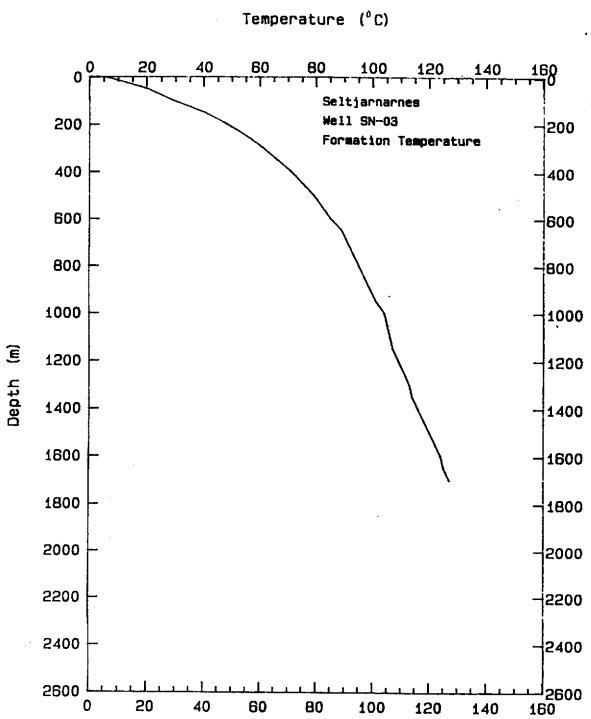

FIGURE 6 Estimated Formation Temperature around Well SN-03

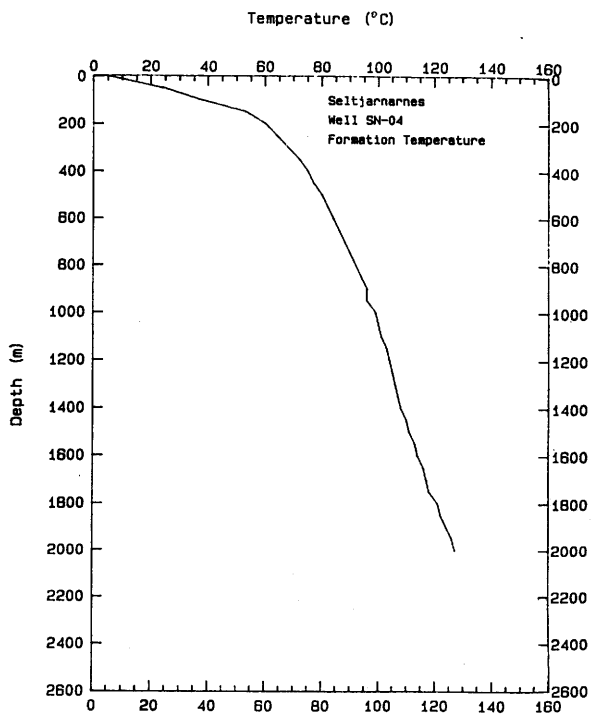

FIGURE 7 Estimated Formation Temperature around Well SN-04

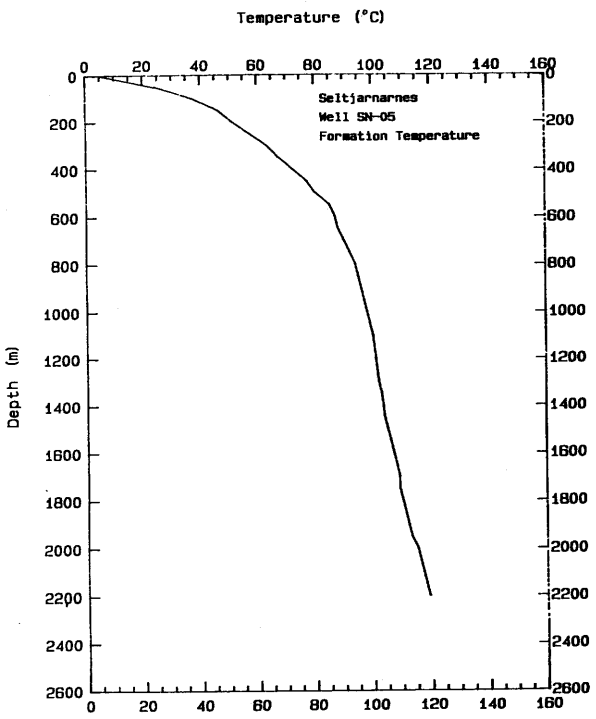

FIGURE 8 Estimated Formation Temperature around Well SN-05

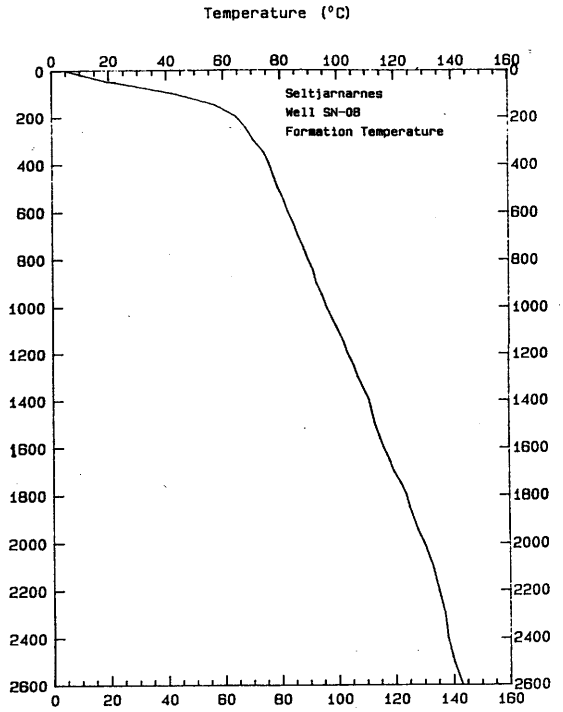

FIGURE 9 Estimated Formation Temperature around Well SN-06

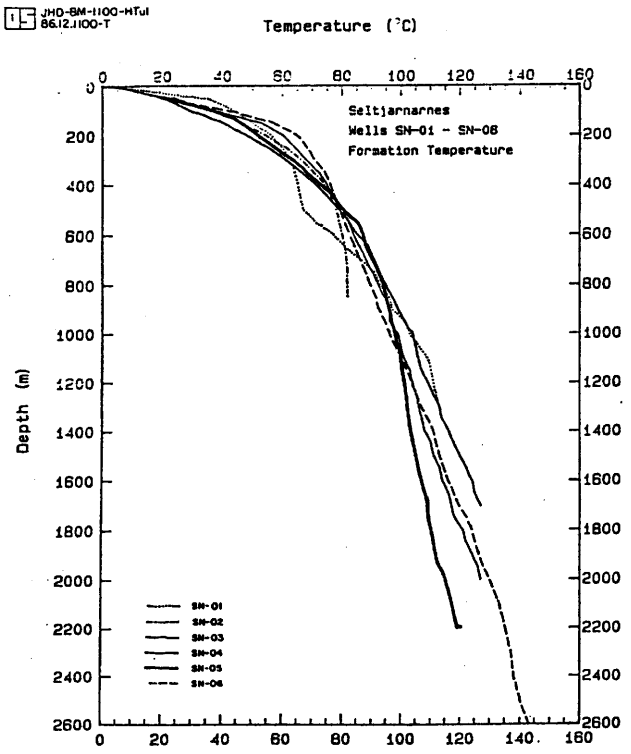

FIGURE 10 Formation Temperature Profiles for Wells SN-01 to SN-06

2.4 Chemistry

Chemical monitoring of the geothermal water has been carried out since 1970, and after the total amount of dissolved solids started in 1981 to increase more rapidly than before the frequency of the chemical sampling was increased. The produced water was rather saline at the beginning of production (1300 ppm total dissolved solids) and barely potable. The salinity increased slowly during the first ten years of production, but soon thereafter the water became unfit for consumption, and heat exchangers had to be installed (Hrefna Kristmannsdóttir, 1983, 1984a, b, c; Hrefna Kristmannsdóttir and Helga Tulinius, 1984; Hrefna Kristmannsdóttir et al., 1984; Jens Tómasson and Kristján Sæmundsson, 1970).

Figures 11 - 14 show the changes with time for the total dissolved solids (TDS), chloride, silica and oxygen-18. The TDS have increased from about 1300 ppm in 1966 up to 2500 ppm - 3000 ppm in 1986. The rate of increase in total concentration varies slightly between individual wells; presently TDS are highest in wells SN-03 and SN-06, but lowest in SN-05. The same is true for the chloride concentration, which is now 1000 ppm - 1400 ppm, but was around 500 ppm in 1966.

The oldest analyses of stable isotopes in the geothermal water are measurements of the D/H ratio from 1967, which are not directly comparable to the more recent $^{18}O/^{16}O$ data. However according to the usual regression line for meteoric water from North Atlantic regions $\delta D = 8\delta^{18}O + 10$ (Craig, 1961), the $^{18}O/^{16}O$ ratios of the thermal water should have been from -15.5 to -10.7 $^{o}/oo$. This is very similar to the present day value and hence no obvious changes can be detected in the isotopic values with time, despite the changes in chemical composition. The data may, however, suggest a slight increase in $\delta^{18}O$ during the year 1984.

The values from well SN-01 demonstrate a decrease in $\delta^{18}O$ with depth. This is most likely because of contamination by local meteoric water ($\delta^{18}O$ = -8.5 $^{o}/oo$) within the uppermost section of the field.

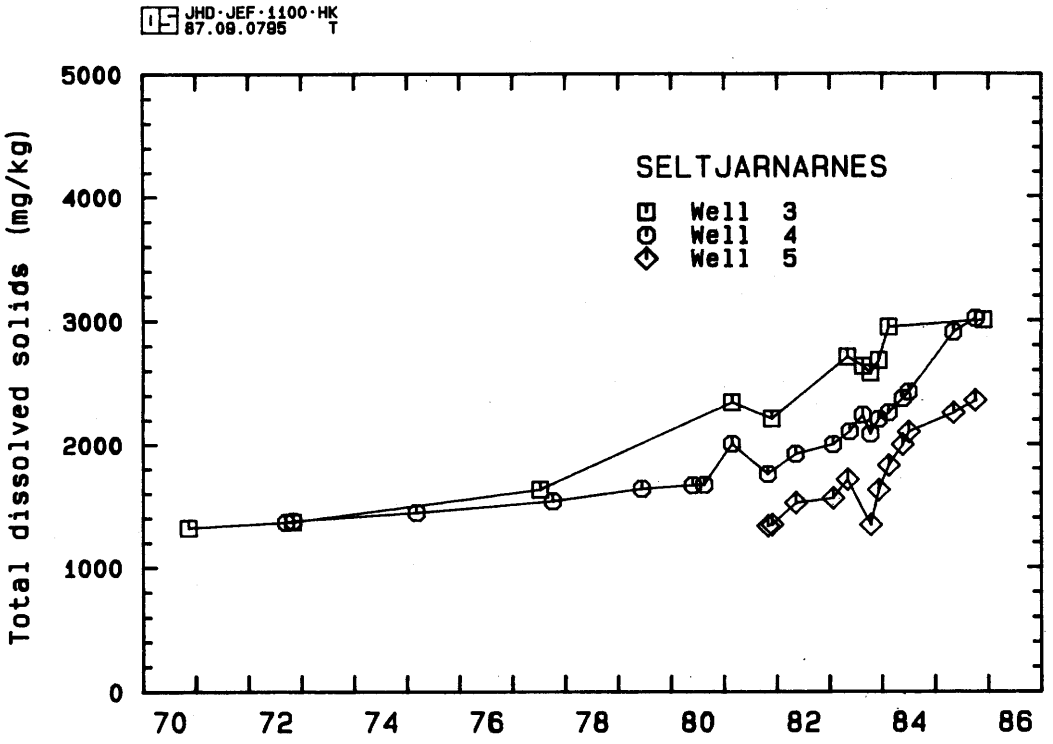

FIGURE 11 Changes in Total Dissolved Solids with Time in Wells in the Seltjarnarnes Field

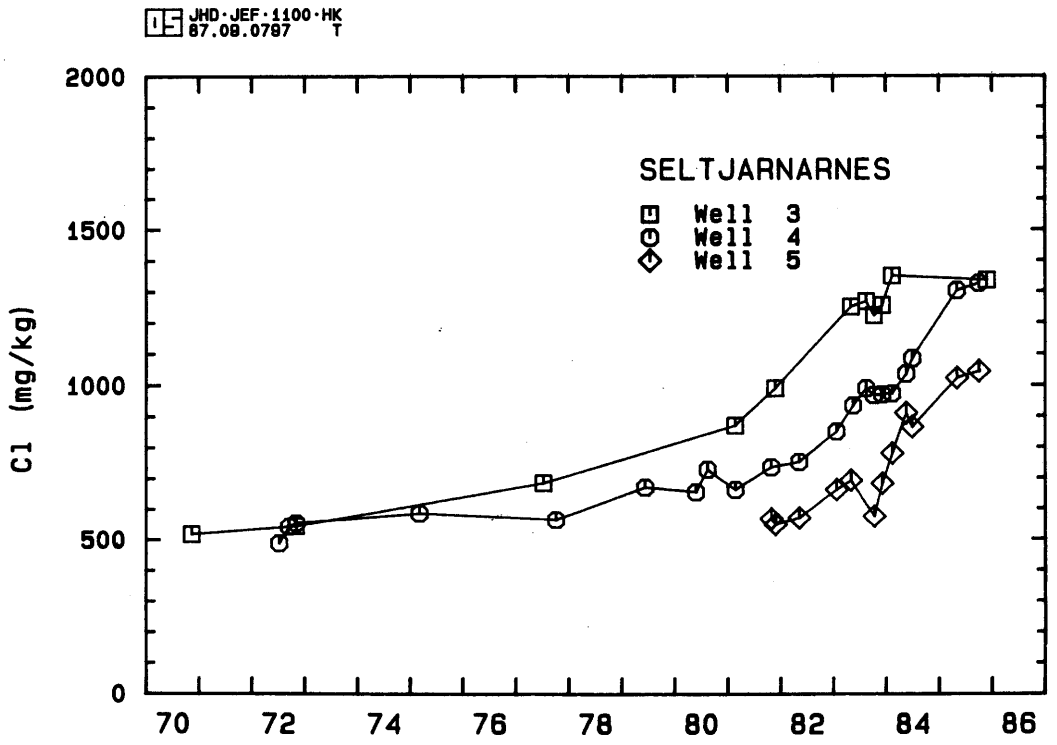

FIGURE 12 Changes in Chloride Concentration with Time in Wells in the Seltjarnarnes Field

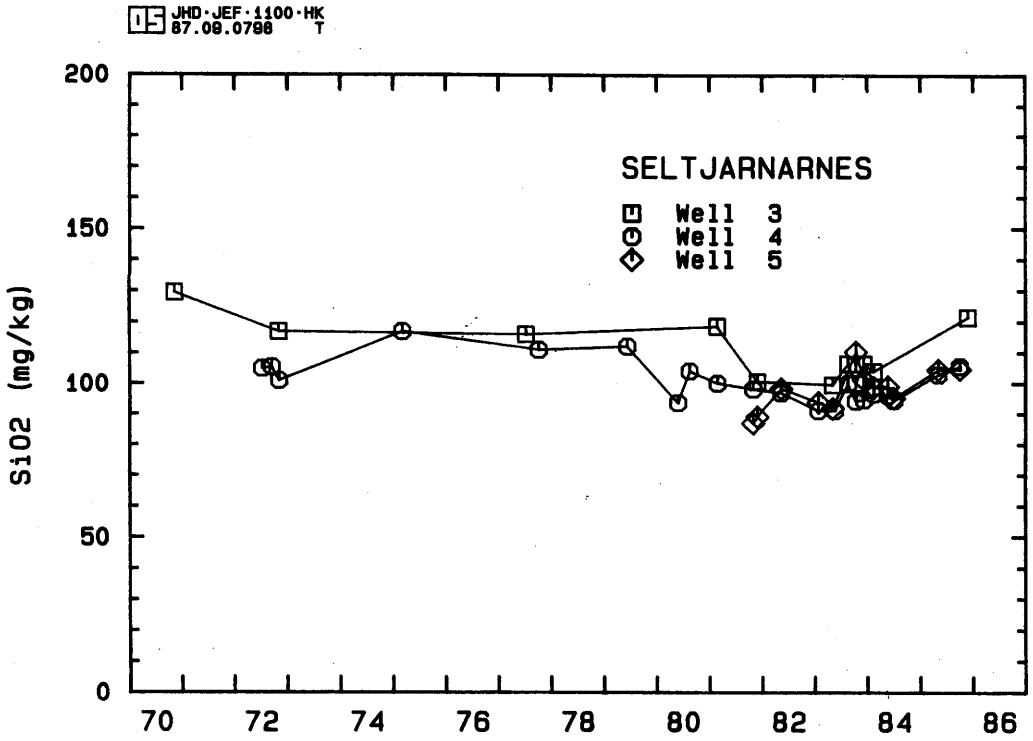

FIGURE 13 Changes in Silica Concentration with Time in Wells in the Seltjarnarnes Field

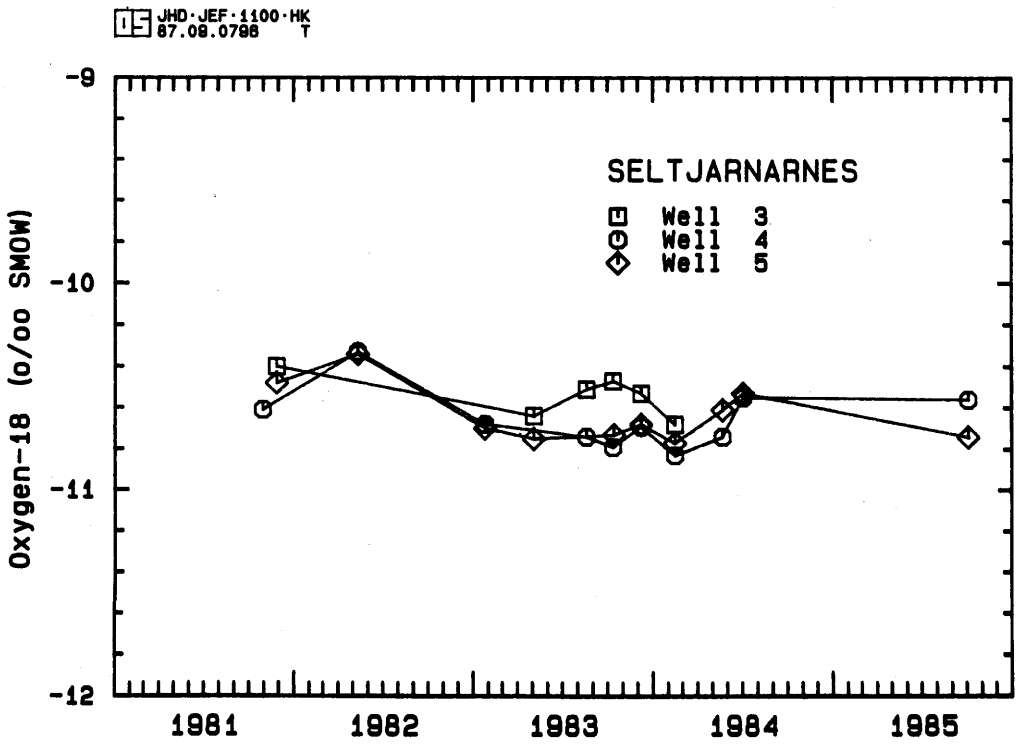

FIGURE 14 Changes in δ^{18} with Time in Wells in the Seltjarnarnes Field

Several downhole samples have been collected and analyzed since 1966 (Figure 15). In wells SN-01 and SN-02 a total of five such samples (four for SN-01 and one for SN-02) were taken in 1966 and 1969. The chloride concentration for all of those samples was similar or around 500 ppm. Samples from well SN-03 taken in 1970, a month after the completion of the well, show higher values above 1000 m depth (732 ppm). This is probably due to contamination by the drilling fluid and the water used in the pressure tests, as other samples taken about a month later show 500 ppm Cl^- at 400 m and 1100 m depths. It therefore appears that the initial chloride concentration was rather uniform over the entire field, around 500 ppm.

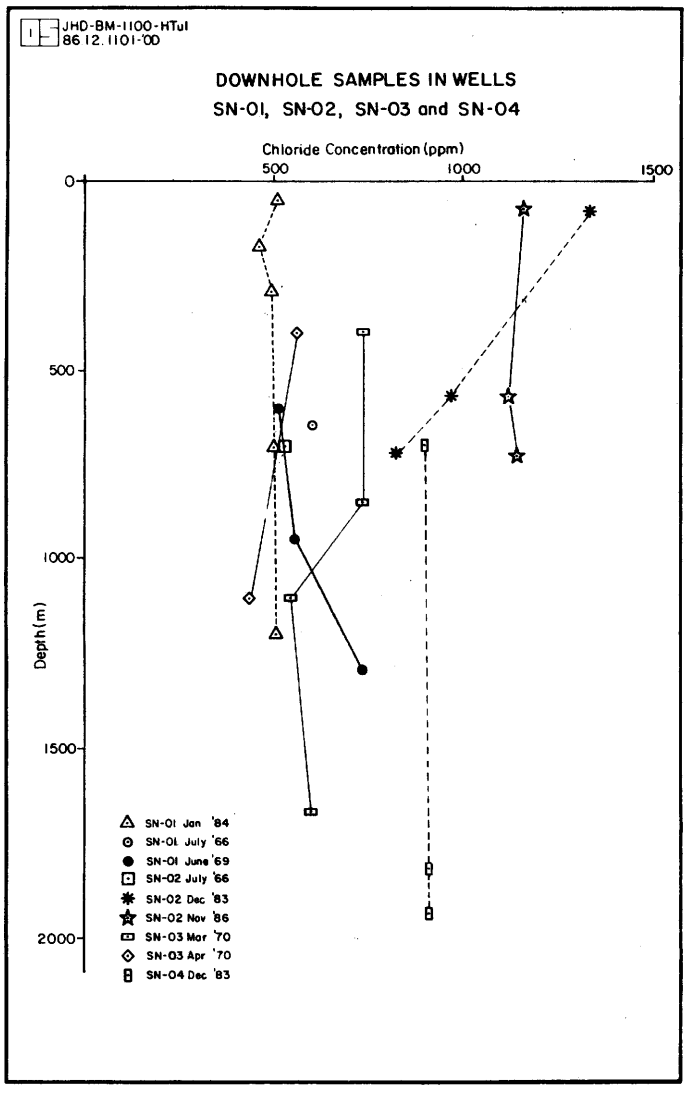

FIGURE 15 Downhole Samples from 1966 to 1986 in Wells SN-01, SN-02, SN-03 and SN-04

Downhole samples taken in well SN-01 in 1984 show that no changes in the salinity have occurred in the vicinity of the well, which most likely lies outside the main reservoir. On the other hand, samples taken in well SN-02 in 1983 show an increase in salinity over the whole depth interval, and the chloride concentration is at present about 1150 ppm over the whole interval. The samples from well SN-04 taken in 1984 also show a considerable increase in Cl^-, and suggest that at that time the cloride concentration in the lower aquifers was about 900 ppm. The concentration of the water produced from the well just before and after the samples were taken showed concentration of 1100 ppm, which suggest that the fluid in the upper aquifers had a chloride concentration of about 2000 ppm.

It is apparent that the salinity of the upper aquifers has increased from 500 ppm Cl^- in 1966 to over 2000 ppm in 1986, probably because of seawater infiltration. The salinity of the lower aquifers has also increased, and is now, 1986, 900 ppm - 1000 ppm Cl^-, also due to recharge of seawater. The fact that the oxygen-18/Oxygen-16 ratio has not increased probably means that the water recharging the system is still mostly of meteoric origin.

The changes with time in some of the dissolved solids indicate that they have reacted with the rock formation before entering the wells.

2.5 Well Testing

The monitoring of the water level in the area started in 1966. In the beginning the main objective was to determine whether the production from the Laugarnes field was causing drawdown in the Seltjarnarnes field, 5 - 6 km away (Jens Tómasson et al., 1977; Þorsteinn Thorsteinsson and Jónas Elíasson, 1970). The production from the Laugarnes field did not have any effect on the water level in the Seltjarnarnes field, at least not for aquifers above 1280 m depth. It was therefore concluded that these two fields are separated by low permeability rocks ("impermeable" barrier; Fig 1); later studies have supported this theory (see Chapter 1).

The water level monitoring in wells SN-01 and SN-02 (Figure 16) continued after production in the field started. After the completion of each well, they were pressurized in an attempt to increase the near wellbore permeability and then injection tests were performed (Þorsteinn Thorsteinsson, 1970a, b, 1985; Þorsteinn Thorsteinsson and Jens Tómasson, 1972; Þorsteinn Thorsteinsson et al., 1985; Árný E. Sveinbjörnssdóttir et al, 1984a, b).

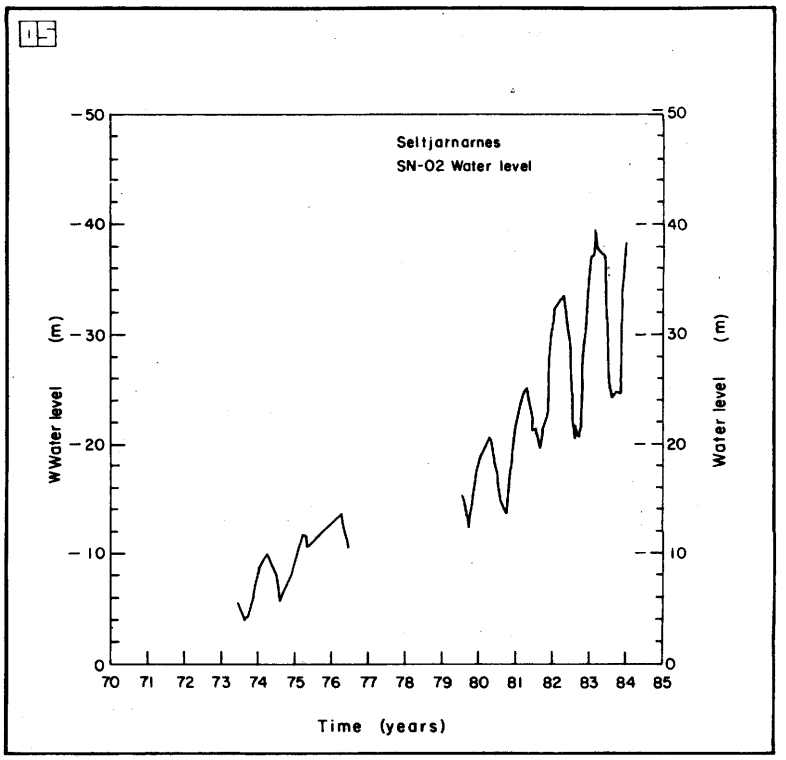

FIGURE 16 Changes in Water Level in Well SN-02 due to Production in Wells SN-03, SN-04 and SN-05 from 1973 to 1984

Table 3 summarizes the results of pressure transient tests in terms of the transmissivity (T) and the storage coefficient (S). Some of the values given in Table 4 are based on interference tests, where the water level was measured in one or more wells, while a different well was flowing or recovering. Other values are derived from build-up tests after a few days of flowing, and the remaining values are calculated from water level drawdown due to production from one or more wells over at least one year. Some of the transmissivity (T) values were given in l/s/m or m^2/s; these values were converted to $m^3/Pa\ s$ for better comparison using the density of 110°C water (957.5 kg/m^3). Permeability values (k) were estimated from the transmissivity (T) assuming a reservoir thickness (h) of 1800 m and the viscosity of 110°C water (2.5×10^{-4} Pa s).

Injection (air and water) and pumping tests have been used to get an estimate of the short term drawdown, h = B*Q + C*Q2, where Q is the flow rate (l/s), and B and C are constants. The constant C indicates the degree of turbulence in the flow. All values of the constants B and C for wells SN-01, SN-03 - SN-06 are listed in Table 4 along with maximum yield for each well. No values of B and C have been published for well SN-02.

TABLE 3 Well Tests in Wells SN-01 - SN-06

Wells p/i+	Wells m+	Depth (m)	T (m^3/Pas)	S (m/Pa)	k (md)	Date	Reference
1	2	500-800	23.4 x 10^{-8}	$4x10^{-9}$	33	Jun 1969	Jens Tómasson et al., 1977 Interference test, water level in SN-02 while pressure test in SN-01
2	2	500-800	13.8 x 10^{-8}		19	1966-1968	Jens Tómasson et al., 1977 Waterlevel changes in SN-01 due to production in SN-02
3	3	100-1700	13-28 x 10^{-8}		29	Mar 1970	Þorsteinn Thorsteinsson, 1970a Build-up after 10 days of flowing
3	1,2	150-1250	11.7 x 10^{-8}	$1-2x10^{-9}$	16	Aug-Sep	Þorsteinn Thorsteinsson, 1970b Interference test
3	3	150-1700	28-57 x 10^{-8}		60	1970	Þorsteinn Thorsteinsson, 1970b Build-up after 14 days of flowing
4	1,2,3	0-1000	11.7 x 10^{-8}		16	May-Aug	Þorsteinn Thorsteinsson and Jens Tómasson, 1972 Water level monitoring in SN-01, SN-02 and SN-03, while SN-04 was flowing and later shut-in
4	1,2,3	1000-1700	31.2 x 10^{-8}		44	1972	Þorsteinn Thorsteinsson and Jens Tómasson, 1972
2,3,4	2		13.3 x 10^{-8}		19	1970-1980	Þorsteinn Thorsteinsson, 1980 Waterlevel changes in SN-02 due to production in SN-02, SN-03 and SN-04
5	5	170-2200	13.2 x 10^{-8}	$19x10^{-9}$	19	May 1981	Þorsteinn Thorsteinsson et al., 1985 Air injection
6	6	414-2540	3.13 x 10^{-8}	$22x10^{-9}$	4	Dec 1984	

+ p/i pumping or injection
+ m waterlevel monitoring

TABLE 4 Calculated Drawdown in Wells SN-01 and SN-03 - SN-06 from well tests

Well	B m/(l/s)	C (m/(l/s))^2	Max yield l/s	Reference
SN-01	0.57	1.05		Jens Tómasson et al., 1977
SN-01	2.0	0.68		Jens Tómasson et al., 1977
SN-03	0.75	0.175	15	Þorsteinn Thorsteinsson, 1970a
SN-04	1.4	0.035	35	Þorsteinn Thorsteinsson and Jens Tómasson, 1972
SN-05	0.5	0.063	30	Árný E. Sveinbjörnsdóttir et al 1984a
SN-06	0.42	0.11	30	Þorsteinn Thorsteinsson, 1985

The curves for the short term drawdown based on the constants in Table 5 are plotted in Figure 17. For well SN-01, which is poor producter, the curve rises very steeply and gives a drawdown of 88 m for 10 l/s production. Well SN-06 yields more than its curve suggests, probably because it had not been cleaned out completely after drilling, when the test was performed.

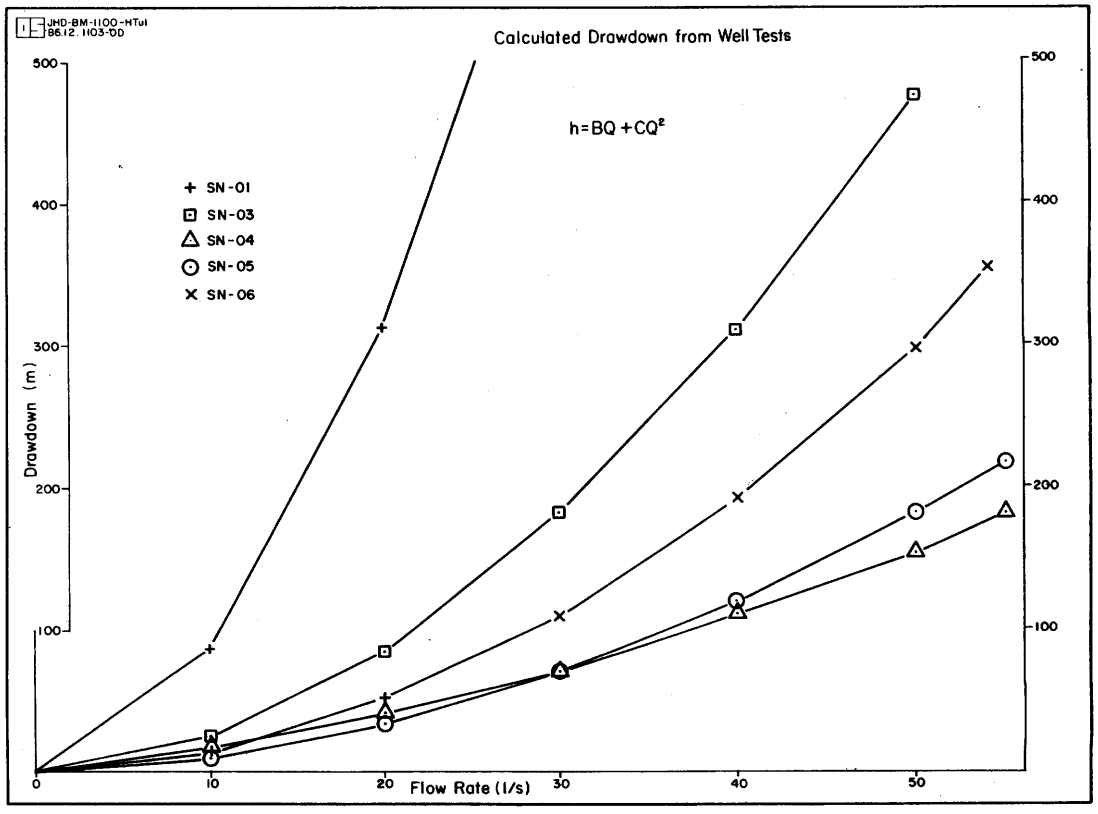

FIGURE 17 Calculated Short Term Drawdown in Wells SN-01, SN-03 - SN-06

As mentioned earlier, several interference tests have been performed. Figure 18 shows data from an interference test performed in August - September 1970, where about 17 l/s were produced from well SN-03 for 14 days, and the water level monitored in wells SN-01 and SN-02 during the production period and for five days after the well was shut in. The drawdown in wells SN-01 and SN-02 over this 14 days period is only 4 m (0.4 bar) in well SN-01 but 6 m (0.6 bar) in well SN-02. Well SN-01 is closer than SN-02 to well SN-03, but experienced less drawdown due to production from well SN-03. This indicates higher permeability between SN-02 and SN-03 than between wells SN-01 and SN-03. A part of the drawdown measured in well SN-02 is, however, attributable to the lowering of its water level due to cooling after the well was shut down for pressure monitoring a day prior to the start up of well SN-03.

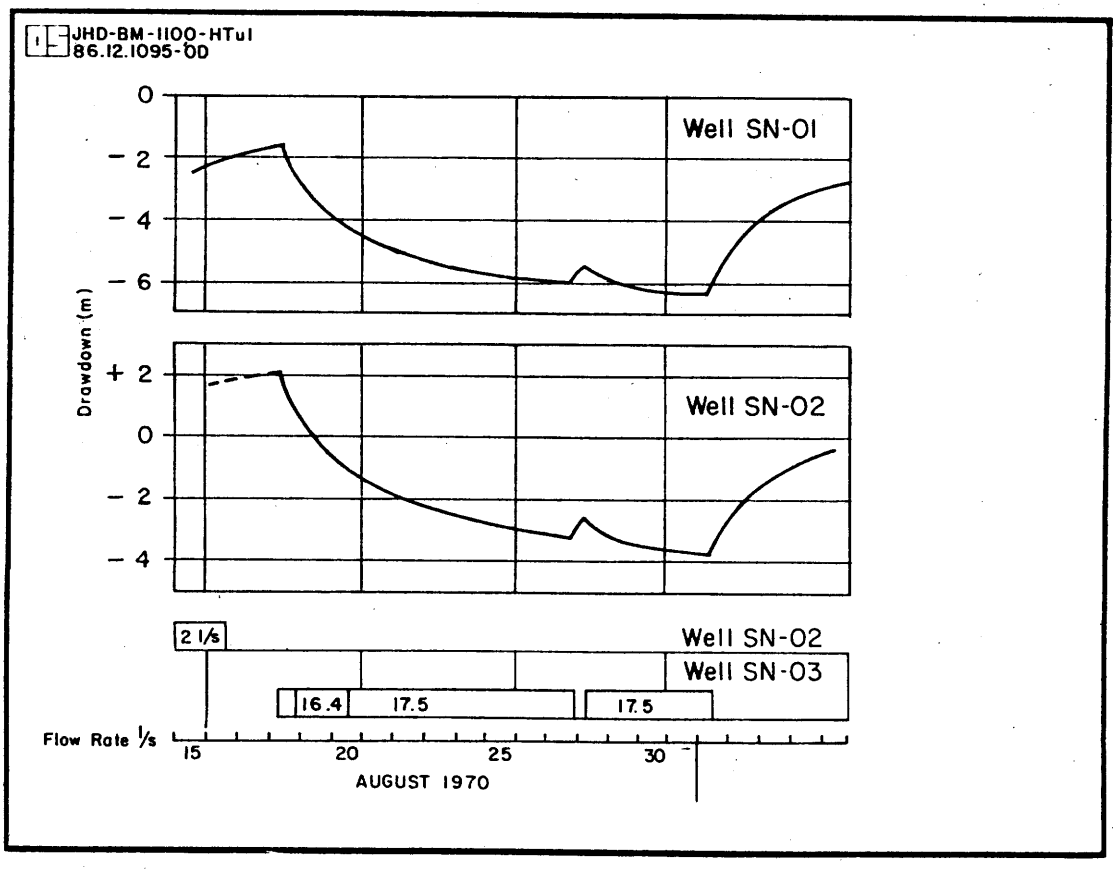

FIGURE 18 Interference Tests in Wells SN-01, SN-02 and SN-03 in 1970

2.6 Production

Fluid production started from well SN-02 in August 1966, and continued until October 1971. The total production from well SN-02 amounted to some 400 million liters. Production from well SN-03 started in August

1970, at a rate of 2-3 l/s. In the winter of 1971-1972 the production from well SN-03 was increased to its maximum production capacity of 17 l/s. The total production from the field was 29 l/s during the summer of 1972, with production from wells SN-03 and SN-04. For the next nine years the production rate was rather stable at 26 l/s during the summer months and 40 l/s during the winter months. Well SN-05 started producing in October 1981 increasing the level of production up to 39 l/s during the summer months and up to 60 l/s during the winter months.

Figure 19 shows the estimated production from wells SN-02 - SN-06 during the period 1967 through 1984. The production from the individual wells was not measured, but has been estimated. The estimated total production for given time periods (summer or winter) was used, and the relative production from each well was estimated on the basis of its maximum capacity and the time period each well was flowing (Figure 20).

The cumulative production is plotted in Figure 21 where it can be seen that the total production from 1966 to 1983 amounts to 1.47 x 10^{10} kg, with a total drawdown of 50 m - 60 m (Figure 16).

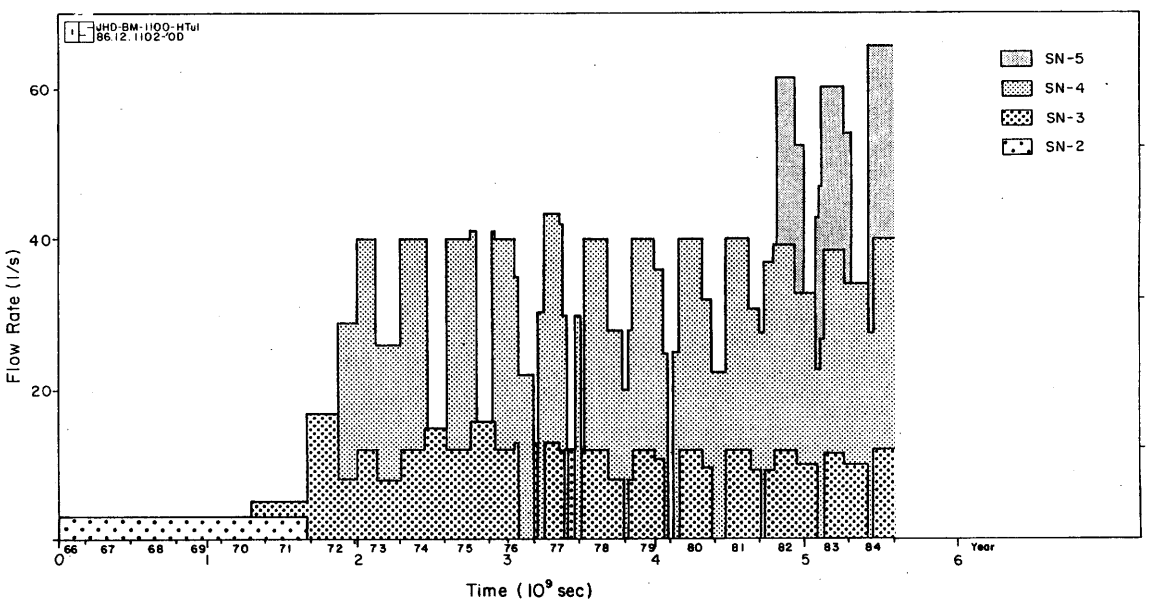

FIGURE 19 Production from Wells SN-02 to SN-05 from 1966 to 1984

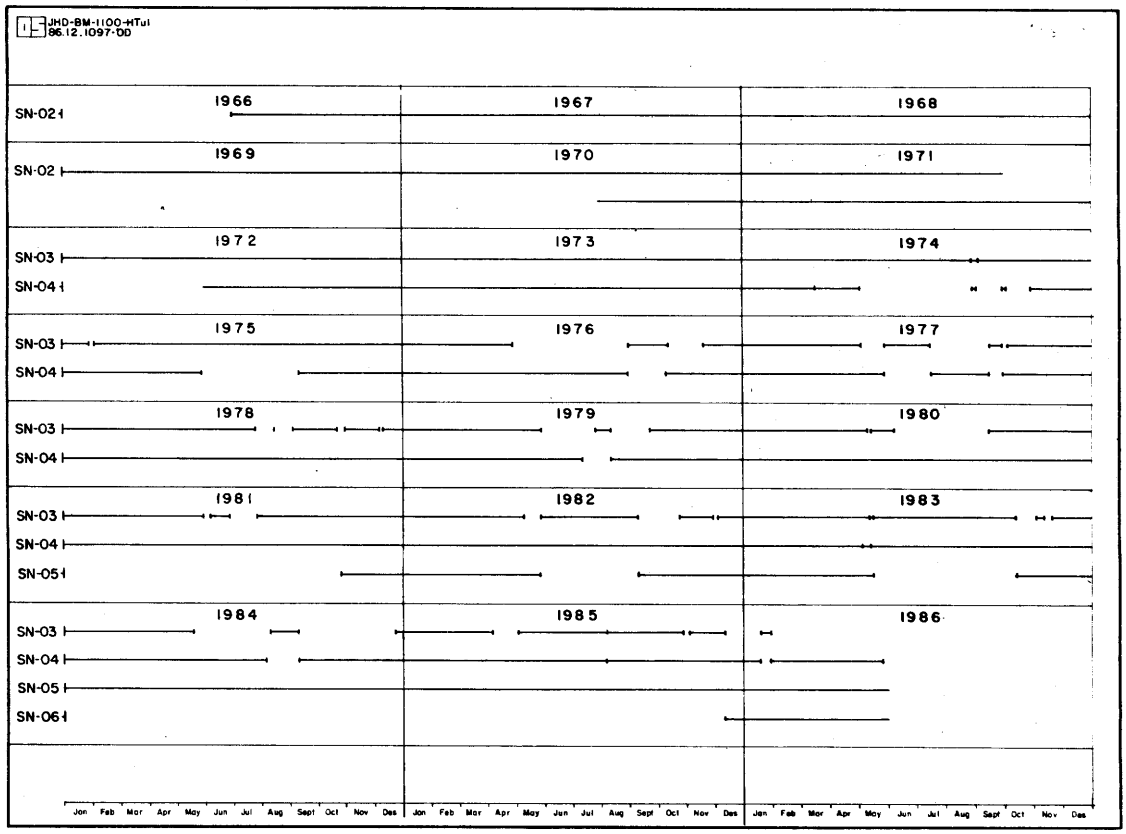

FIGURE 20 Production Times for the Wells

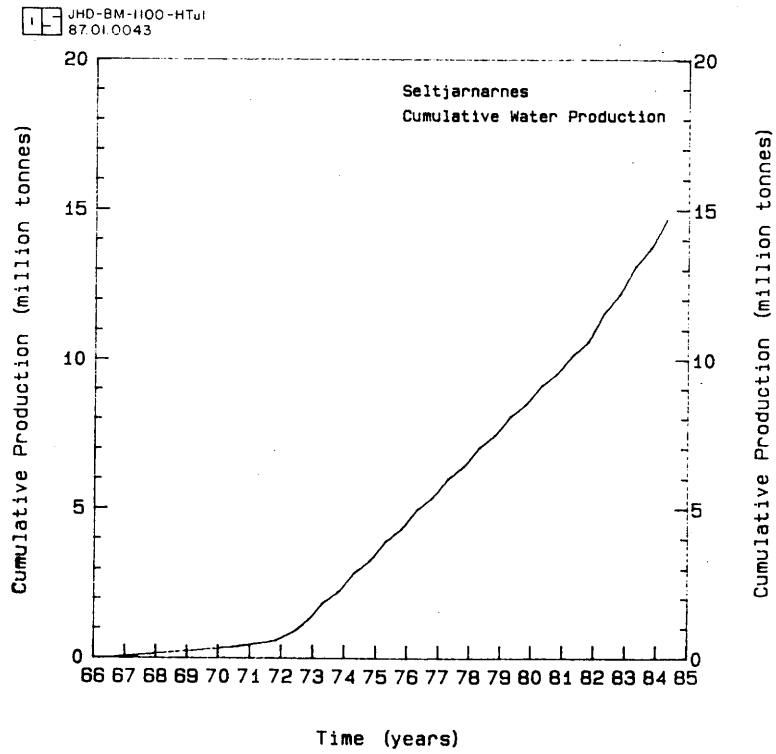

FIGURE 21 Cumulative Production

2.7 Well Logging

All of the wells have been logged using caliper tool, except well SN-03. Resistivity logs have been taken from wells SN-01, SN-02, SN-04 and SN-06 and gamma and neutron-neutron logs are available for the upper 400 m in well SN-06. Analysis of some of these logs have been published (Svanbjörg H. Haraldsdóttir, 1984a, b, c; Árný E. Sveinbjörnsdóttir et al., 1984).

A comprehensive study of the well logs has not been performed so far; it is therefore difficult to get an overall picture of the subsurface resistivity structure.

3 CONCEPTUAL MODEL

After intergrating all the available data from the different disciplines, a conceptual model of the field can be developed. The stable isotope measurements suggest that the geothermal water in the Seltjarnarnes field has a different origin from the geothermal water in the nearby fields Laugarnes and Ellidaar. The thermal gradient low between these fields and the fact that no pressure changes were detected in the Seltjarnarnes field due to production in the Laugarnes field, indicate the presence of low permeability rocks (faults?) between these fields. This inferred permeability barrier is the only field boundary that can be detected from the available data.

The isotopes also indicate that the water is meteoric in origin, infiltrating from the highlands tens of kilometers to the north. The water percolates down, probably to about 3 km - 4 km depth. The water flows to the south and heats up due to the anomalous thermal conditions in the subsurface rocks, then ascends under the Seltjarnarnes field through fissures that extend to considerable depth and are more permeable than the surrounding areas. The oxygen-18/oxygen-16 ratio suggests that a large portion of the fluids recharging the field during exploitation are meteoric.

The increase in the concentration of most chemical components of the produced water indicates that a portion of the recharge fluids consists of highly saline water. The source is probably

1) seawater recharging from the southwest into the reservoir at shallow levels (above 400 m), with percolation of the saline fluids to deeper aquifers,
2) on the recharge fluid has acquired its chemical composition by passage through old marine sediments of hyaloclastite.

Most of the aquifers are located in the interval from about 400 m to 2200 m depth.

Figure 22 shows a top view of the Seltjarnarnes area. Lines with equal thermal gradient in the uppermost 200 m - 300 m are plotted in the figure along with suggested flow directions for the recharge water (plotted as arrows).

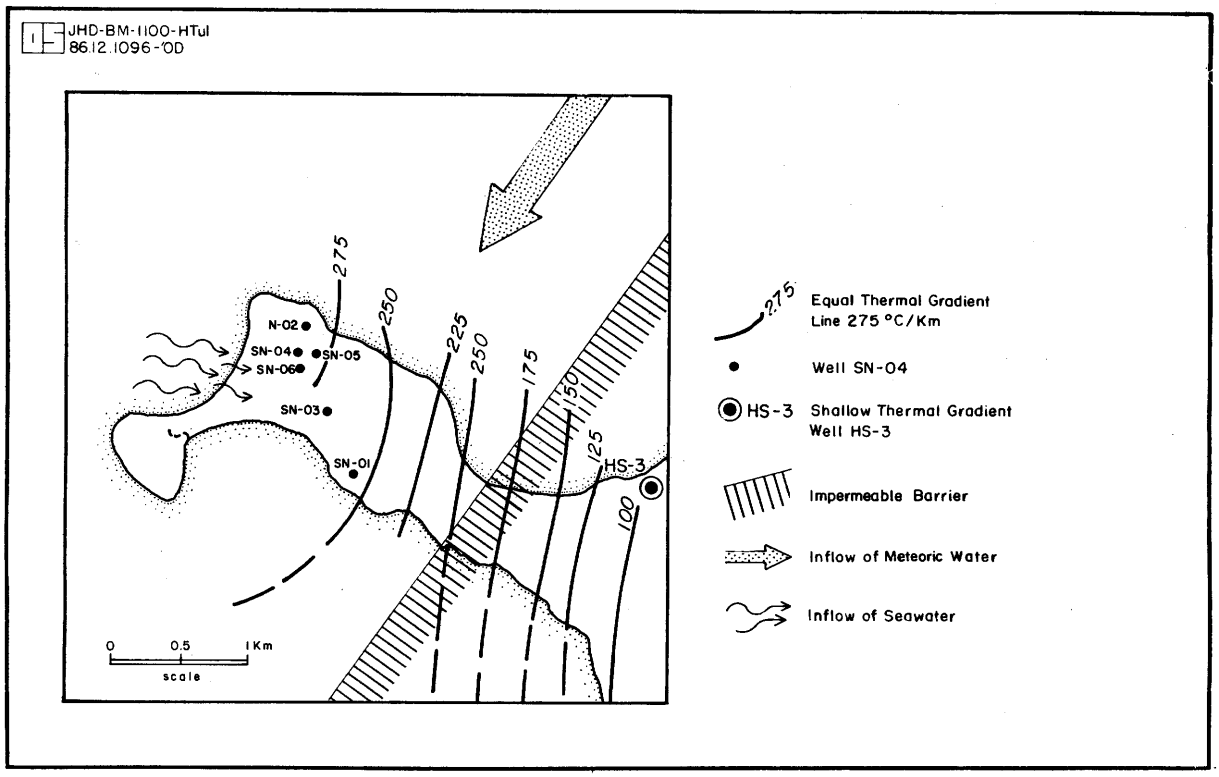

FIGURE 22 Conceptual Model of the Seltjarnarnes Area

4 NUMERICAL SIMULATION

4.1 The Computer Programs

The single-phase near-isothermal numerical code PT (Guðmundur Böðvarsson, 1981)(for Pressure and Temperature) was used to simulate the interference tests and the production history. The simulator is three-dimensional and solves the mass and energy transport equations for a liquid-saturated, heterogeneous, porous and/or fractured medium. It uses the "integrated finite-difference method" for discreting the medium and formulating the governing equations (Edwards, 1972). The set of linear equations is solved at each time step by direct means with an efficient sparse matrix solver (Duff, 1978).

The simulator allows for temperature - and/or pressure dependent fluid and rock properties. The fluid density is calculated as a function of pressure and temperature with a polynomial approximation accurate to within 1%. Fluid viscosity is calculated as a function of temperature with an exponential expression accurate to within 1%. The simulator has been validated by many analytical solutions as well as by field experiments (Gudmundur Bodvarsson, 1981).

A modified version by Lai (1985), and Spencer (1986) was used to model the changes in chloride and silica concentration, and oxygen-18/-oxygen-16 ratio. The program is an integrated pressure-temperature--chemistry numerical code capable of modeling two-dimensional fluid, heat and chemical transport in fractured porous media. A combination of a second order Godunov method and operator splitting is utilized to solve the convection-diffusion type equations.

4.2 Numerical Model

In the first attempt to match the interference and production data, a two-dimensional model (horizontal flow) was used. It is useful to start with a simple model and investigate how well it can match the available data. In this way complexities that illustrate the shortcomings of a two-dimensional model may be identified and addressed in subsequent modeling studies.

In the beginning isothermal conditions were simulated with temperature kept constant at 110°C and only the mass balance equation used. A model was used with a 1800 m thick recharge layer representing the depth interval 400 m - 2200 m. The initial average pressure was estimated to be 123 bars, using the average depth of 1300 m, density of

water at 110°C, and the initial wellhead pressure in well SN-02 of +13 m a.s.l. Later nonisothermal case was used. Table 5 lists the values of the parameters used in the simulation, both for the isothermal case (Table 5a) and for the nonisothermal case (Table 5b)

TABLE 5 Parameters Used in the Simulations

a) Two dimensional, mass balance only (constant temperature)

Parameter	Value
Fluid pressure	123 bars
Initial temperature	110°C
Density of the solids	2650 kg/m^3
Specific heat of the solids	1000 J/kg/°C
Thermal conductivity	2 W/m°C
Specific heat of the fluid	4200 kJ/kg°C
Fluid viscosity	calculated from temperature
Fluid compressibility	calculated from pressure and temperature
Fluid density	calculated from pressure and temperature

b) Energy and mass equations used (variable temperature)

Parameter	Value
Initial pressure	123 bars
Initial temperature in the field	110°C
Initial temperature outside the field	75°C
Density of the solids	2650 kg/m^3
Specific heat of the solids	1000 J/kg/°C
Thermal conductivity	0 W/m°C
Specific heat of the fluid	4200 kJ/kg°C
Fluid viscosity	calculated from temperature
Fluid compressibility	calculated from pressure and temperature
Fluid density	calculated from pressure and temperature

The mesh used consisted of squares 50 m x 50 m in size around the wells, increasing in steps of 2 x 2 up to about 100 km x 100 km for the largest and farthest away nodes (Figure 23). The grid extended far enough in all directions that boundary conditions were not felt during the simulation (infinite reservoir system). The total number of elements was 316.

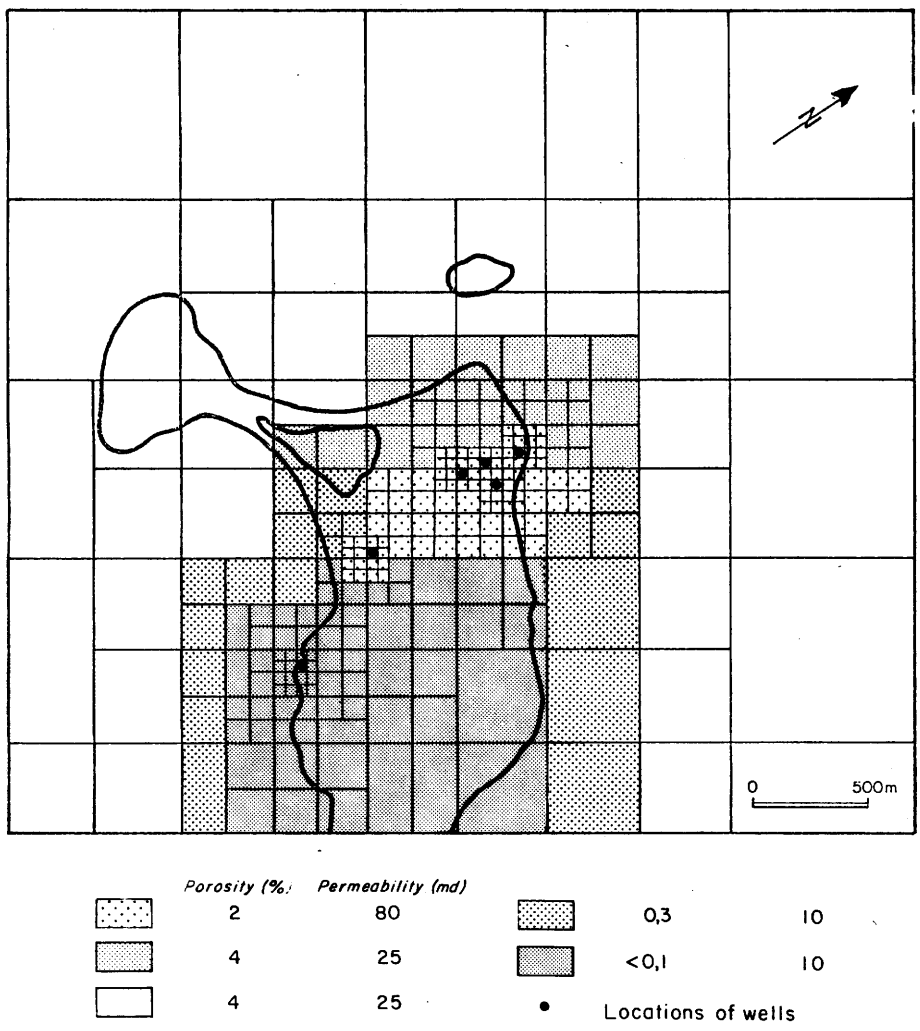

FIGURE 23 The Mesh Used in the Simulation and the Permeability and Porosity Regions

The interference tests (Figure 18) involving wells SN-01, SN-02 and SN-03 in August - September 1970, and the production history (Figure 19), were simulated. Trial and error simulations were carried out using permeability and storativity as adjustable parameters. It was assumed that the storativity of the model was only because of the compressibility of the water + rock, or storativity; $\phi C_t = \phi C_r + \phi C_w$ where ϕ is porosity, C_t is total compressibility and C_w and C_r are the compressibilities of the water and rock, respectively. The compressibility of the rock was held constant at 5×10^{-10} Pa^{-1}. Excess drawdown due to cooling in well SN-02 during the interference test was, however, not taken into account.

The permeability primarily affects the magnitude of the pressure drawdown for a given well production. The porosity affects the pressure transients in somewhat different way. The porosity primarily affects the time response of the system to changes in production. The lower the porosity the faster the response. The porosity effects are most pronounced in pressure build-up after production.

4.3 Simulation Results

The best model derived from the match using the interference test data (Figure 24) consisted of 6 regions with different porosities and permeabilities. In the model the area around all the wells except SN-01 (area 5) had the largest permeability, or k = 80 md and a porosity of 2% (Figure 23). The total surface area and volume of this region (region 5) is about 0.5 km^2 and 0.8 km^3, respectively. The area around well SN-01 (region 1) had the lowest porosity or <0.1%, and a permeability of 7 md. In the model the porosity increases away from the wellfield with a value of 15% 4 km away (region 4); reprecenting recharge reservoir with a large storativity. The permeability of this area is about 10 - 15 md. The porosity and permeability near the wellfield are estimated to be 3% and 10 md, respectively (region 2).

To match adequately the pressure transients for both wells other parameter values in different regions had to be used. In the model the porosity between region 1 (well SN-01) and region 2 is around 0.3%, with a permeability of 10 md. Region 6 has a porosity of 4%, and a permeability of 10 md.

The match with the data from the injection test was not perfect, which may be explained by fracture effects (Guðmundur Pálmason et al., 1983) not taken into account in our model. Another possible explanation is three-dimensional effects.

After matching the interference data the model had to be modified slightly to get a good match for the production history (Figure 25). The permeability away from the wellfield (regions 2, 4 and 6) had to be increased to 17 md, and the porosity in the regions next to the wellfield (region 2) was increased from 3% to 4%, with other model parameters remaining the same.

The fact that somewhat different models were needed to get good matches with both the interference test data and the production history suggest that fracture effects may be important. The interference test lasted for only 14 days such that the permeability due to fractures was probably dominant, but for the 16 year production history the time was long enough such that the matrix permeability had significant effects on the pressure transients.

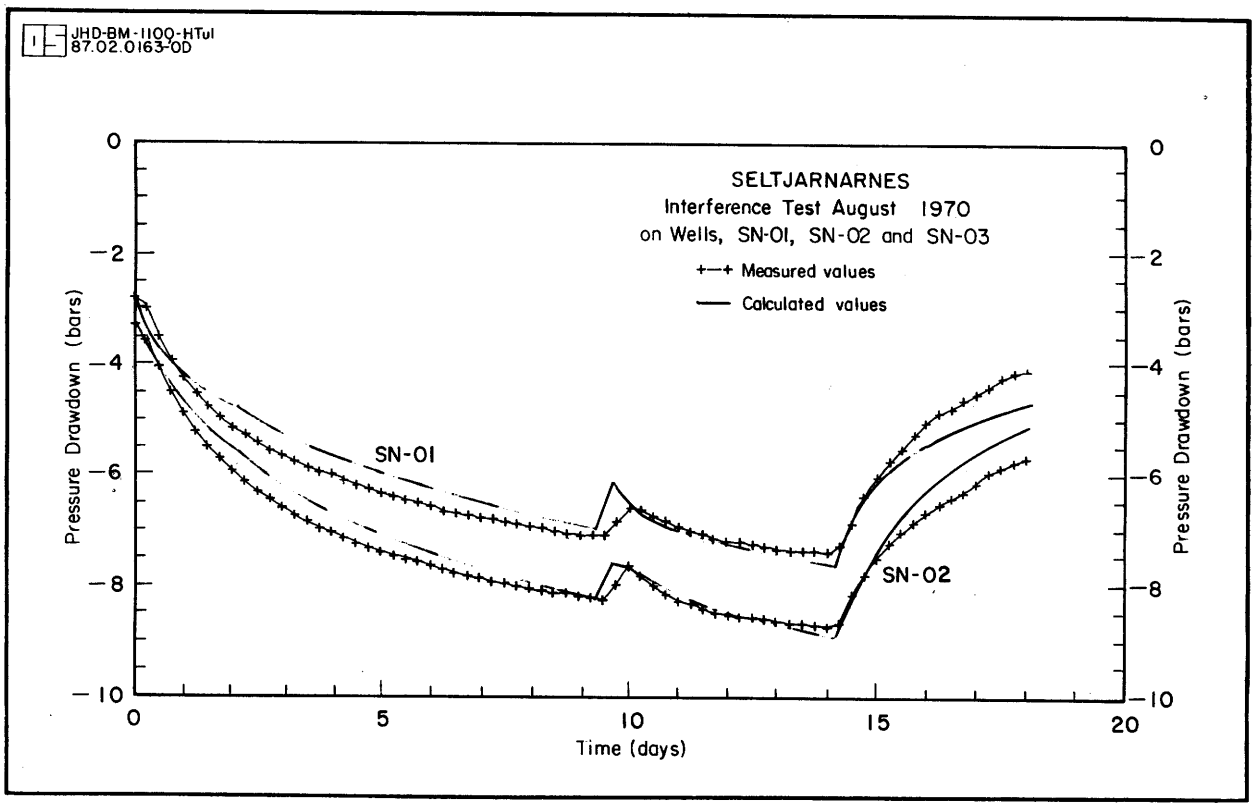

FIGURE 24 Interference Tests, Data and Calculated Curves

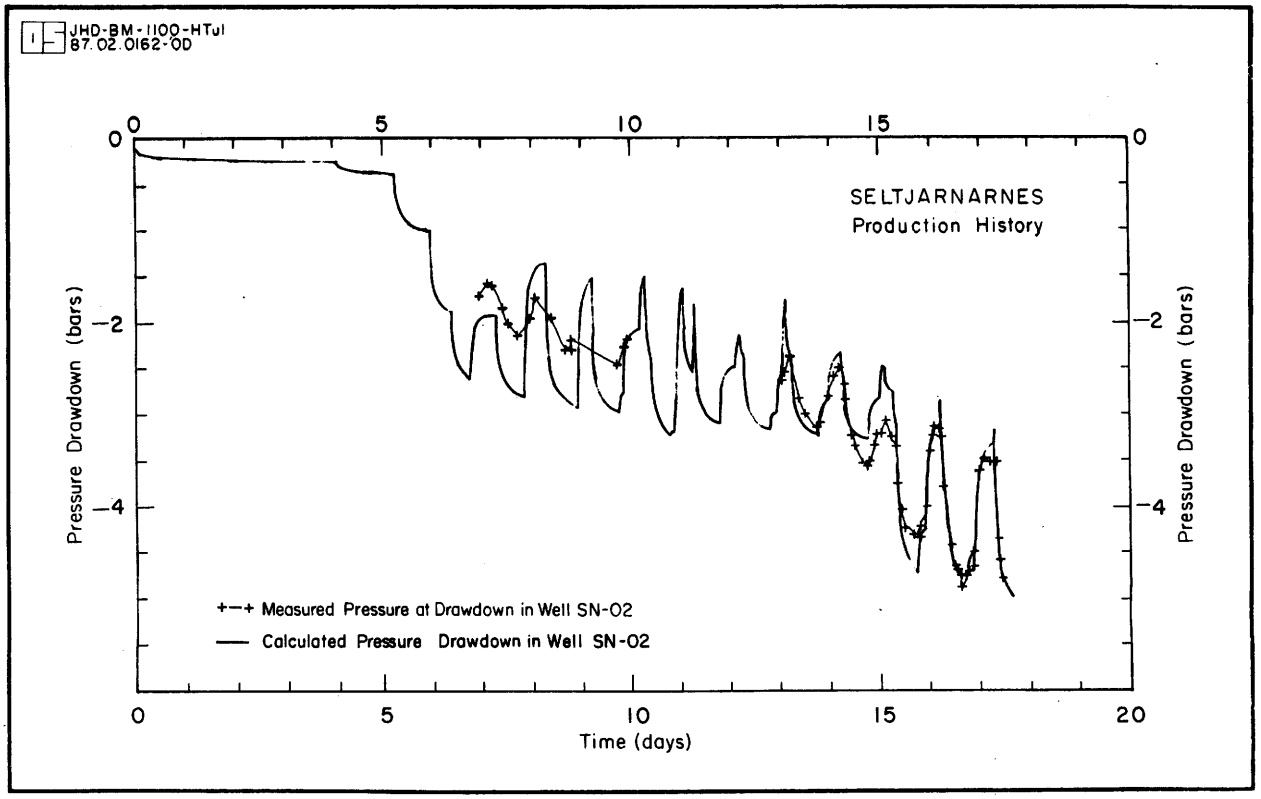

FIGURE 25 Production History, Data and Calculated Curves

4.4 Sensitivity studies

When a rather complex distribution of porosities and permeabilities is necessary to match pressure transient data, one always wonders how unique these distributions are. We conducted sensitivity studies on the estimated porosities and permeabilities primarily with the objective of trying to reduce the number of parameter values needed. This attempt was not successful as all of the parameters simplifications tried yielded worse matches with the observation data than those obtained by the best model. We believe that, given the rather simple two-dimensional porous media model, the transmissivity (kH) distribution determined is close to the effective water/matrix transmissivity in the actual reservoir rocks.

The estimated porosity values are much more in question, as one can only estimate the total storage or CH, rather than the porosity perse. In the modeling we use a confined system where the storage is controled by the compressibility of the rock + water, whereas in the actual system the storage may be dominated by unconfined (free water table) conditions in parts of the reservoir, or by fracture compressibility. This would in turn reduce the porosity values determined from the matches with the data.

Other ambiguities with matching only pressure transient data lie in the uncertaintities regarding the effective reservoir thickness. An identical match with the data can be obtained by scaling the reservoir thickness, permeability and storativity (Ø·C). For example, the same match can be obtained using 18 times lower reservoir thickness (100 m) and increasing all permeabilities and compressibilities by the same factor. More accurate determination of the actual reservoir thickness, permeability, porosity and compressibility can only be achieved if other transient data are also matched, such as temperature and/or chemical changes in the produced fluids. This will be addressed in the next section.

4.5 Chemistry and Temperature Match

After obtaining a match using only the mass balance equation, the temperature was taken into account and the energy equation used. The available temperature data is not reliable enough to determine whether any cooling has occurred in the field. It is, however, apparent that very little cooling if any has occurred; at most 2°C in well SN-02 over several years. The same grid was used as before (Chapter 4.2) and the volume divided into two regions, a high temperature one with an initial temperature of 110°C, and a low temperature region with a

temperature of 75°C. The high temperature region includes the well-field (region 6 and well SN-01). Using this temperature distribution, very little cooling was calculated in the field (less than 1°C) over the production history. This is probably less cooling than has actually accurred in the field which could mean either that the high temperature region is too large or that the temperature in the low temperature region should be lower, but as mentioned earlier the temperature data is not good enough to obtain better match.

The next step was to match the chemistry changes in the wells. Based upon the available data, a simple model of the field was developed. In the beginning, a simple two-layer mesh, in a vertical plane, was employed. The regions directly above and adjacent to the hot field were assumed to contain fluid of nearly the same composition as that initially present in the geothermal reservoir (chloride = 500 ppm, sodium = 300 ppm). The silica concentrations in the top and side regions were the equilibrium values at the assumed temperatures of each zone and the oxygen-18 content was slightly less in the lower recharge zone. Figure 26 shows a sketch of the mesh and the initial concentrations and temperatures. The temperatures of the different zones were derived from well data.

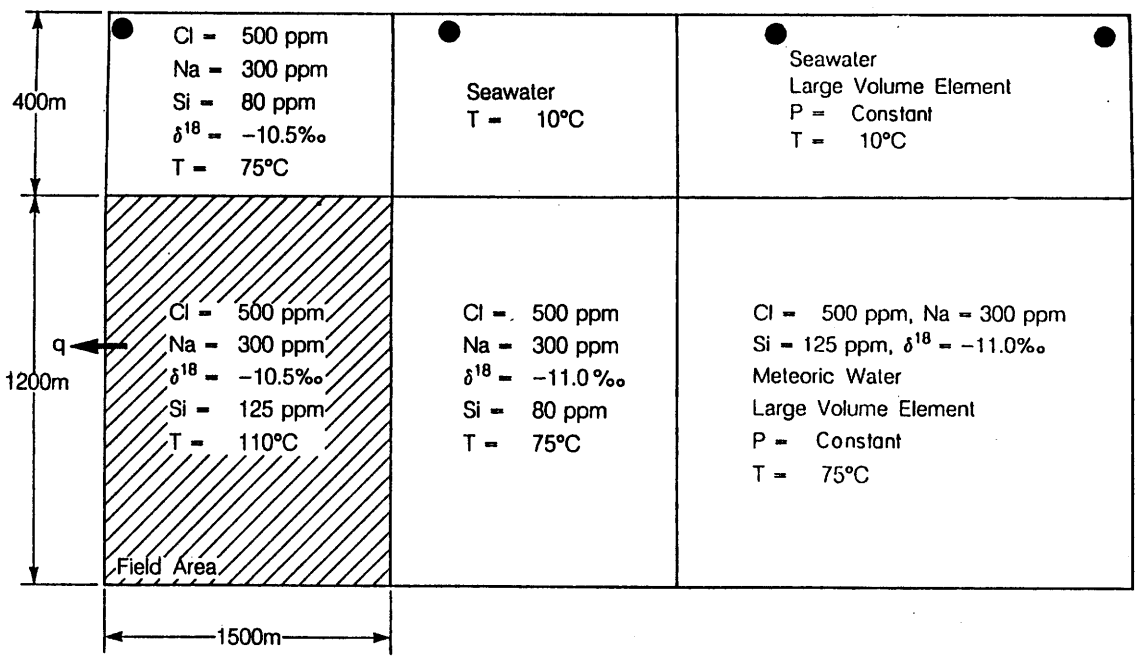

FIGURE 26 Simple Model of the Seltjarnarnes Geothermal Field

Using a trial and error procedure a match for the data was obtained. Figures 27-30 show the field data plotted against time for silica, chloride, sodium and oxygen-18, along with the computed results obtained from the numerical model. Due to the wide scatter of the field data, it was difficult to determine accurately the field parameters inferred from the match. The results obtained suggest that a reservoir volume between 7.5×10^8 m^3 and 1.0×10^9 m^3 and a porosity between 2% and 5% was necessary to match the model data. The matches shown in the figures were obtained with a model having a reservoir volume of 7.5×10^8 m^3, a porosity of 2% with 82% of the recharge into the field coming from the side region which is less saline than seawater. This model was chosen as the best match as it was the only model within the ranges of volume and porosities given above, to show no increase in the oxygen-18 over time, in agreement with the field data. The lower porosity and smaller volume required less recharge from the more saline top and more recharge from the side. The values for A/V (surface area open to reaction per volume of system) and (average grain radius) were found to be 1.0 m^{-1} and 0.35 m, respectively, in all the matches made with models having reservoir volumes and porosities within the ranges given above. The low value for A/V (and therefore high value for ω) indicates that the kinetic reactions of silica and oxygen-18 play a relatively small role in this system. To illustrate this point, a plot (Figure 31) with silica concentration versus time was made for two cases: with kinetic reactions and without (convection only), using the "best match" model.

It must be emphasized that due to the use of such a coarse mesh, the model gives only rough estimates of the field parameters and flow patterns. The close agreement of the volume and porosity estimats for the field region obtained by a pressure and temperature data match, with the results of the simple two-layer model found by the chemical transport match, lends support to the value of chemical transport modeling. To further delimit the field parameters, a finer mesh must be designed. This was the next step taken in modeling the Seltjarnarnes field.

The finer mesh (Figure 23) described above (Chapter 4.2), along with the parameters based on the temperature and pressure match and available chemical field data, were employed in further study of the Seltjarnarnes field. The initial conditions for the chemistry of the fluid in the wellfield region were set by field data obtained at the initiation of field production. Two different fluid chemistries were incorporated in the model, representing seawater and meteoric water.

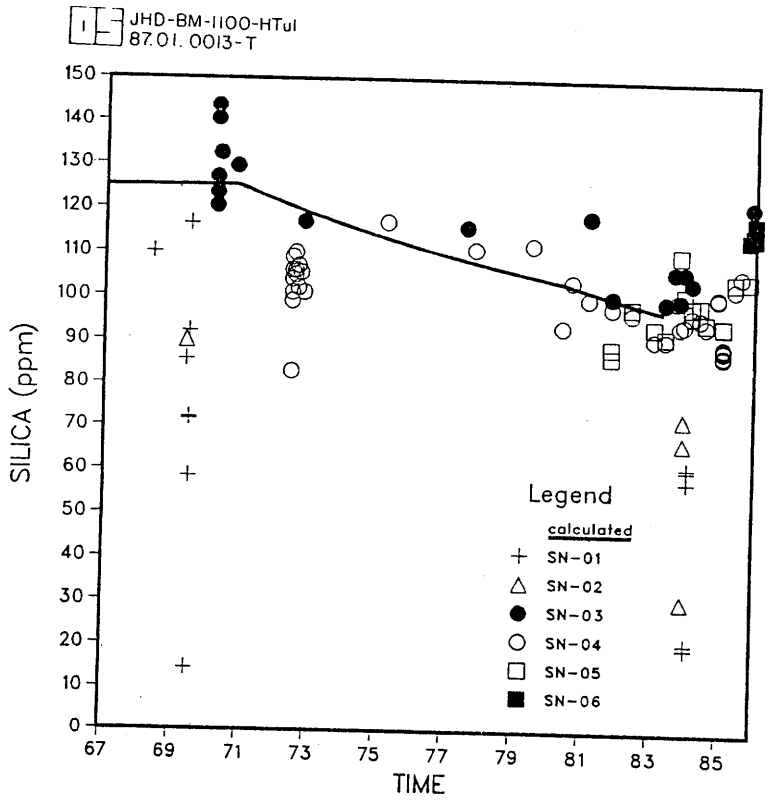

FIGURE 27 Plot of Silica versus Time Showing the Match between the Simple Numerical Model and Field Data. Using the Simple Model

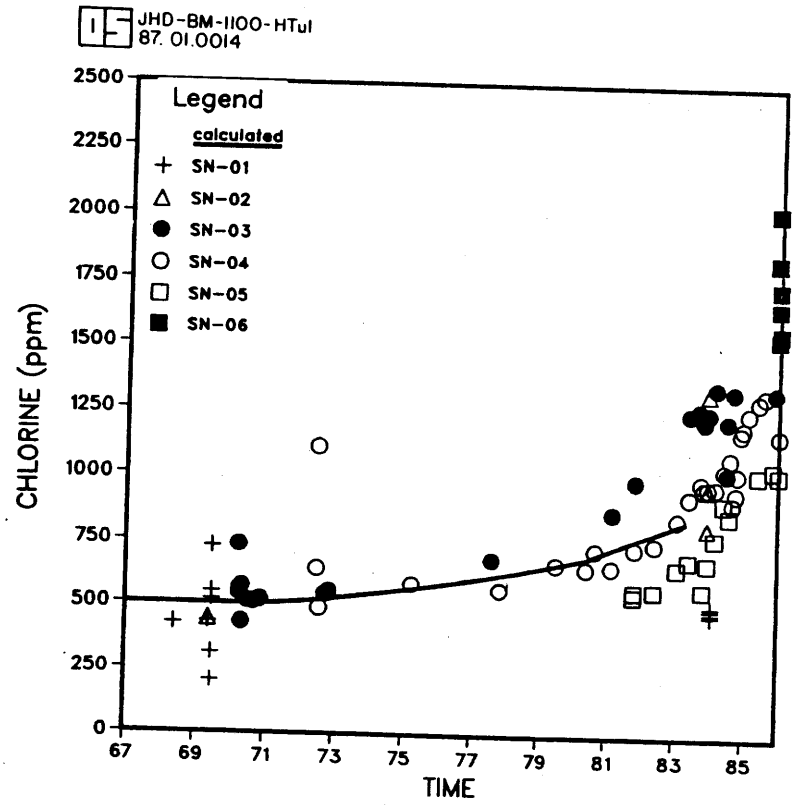

FIGURE 28 Plot of Chloride versus Time Showing the Match between the Simple Numerical Model and Field Data. Using the Simple Model

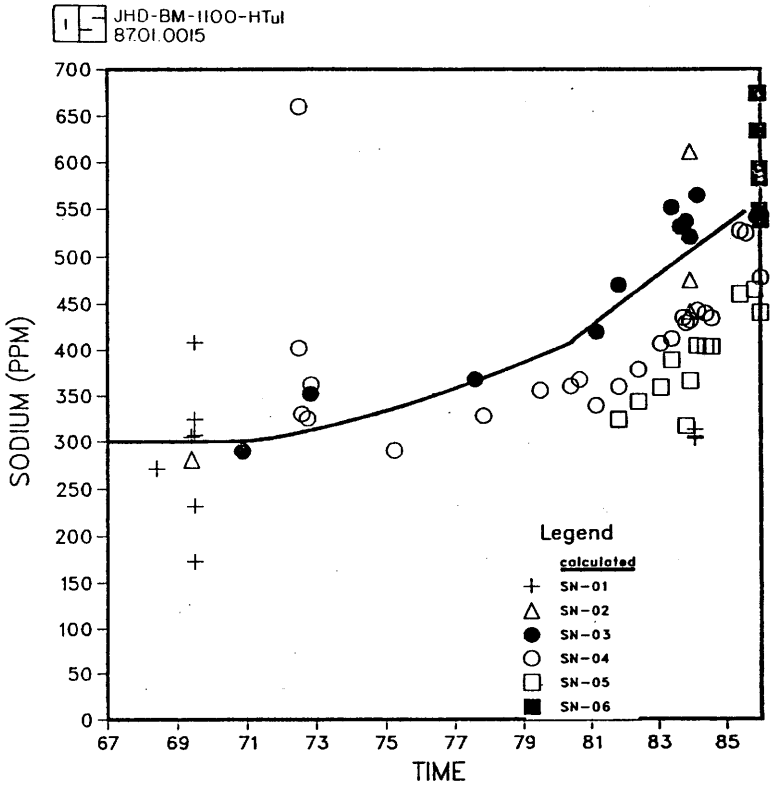

FIGURE 29 Plot of Sodium versus Time Showing the Match between the Simple Numerical Model and Field Data. Using the Simple Model

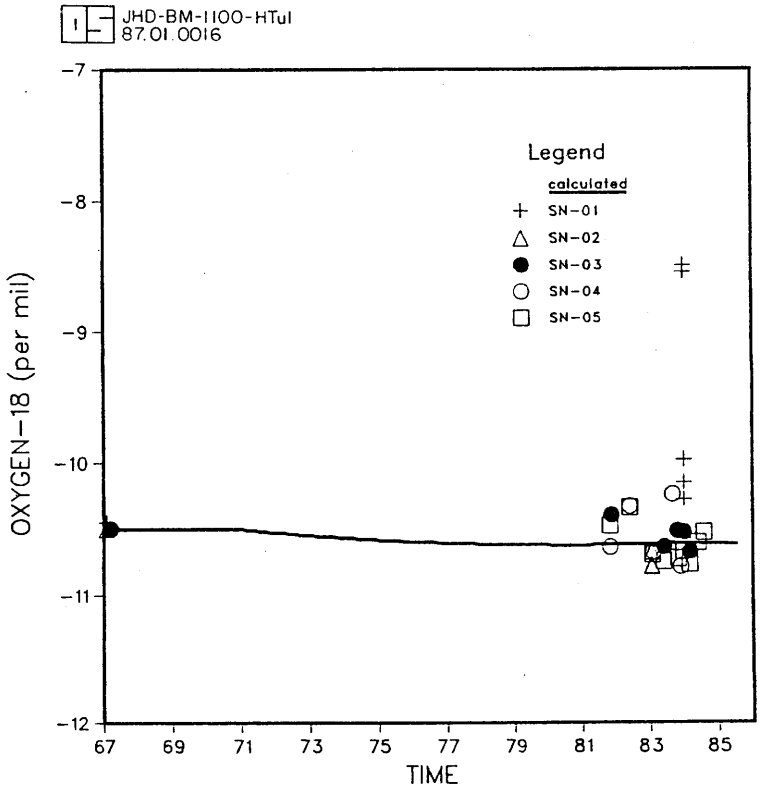

FIGURE 30 Plot of Oxygen-18 versus Time Showing the Match between the Simple Numerical Model and Field Data. Using the Simple Model

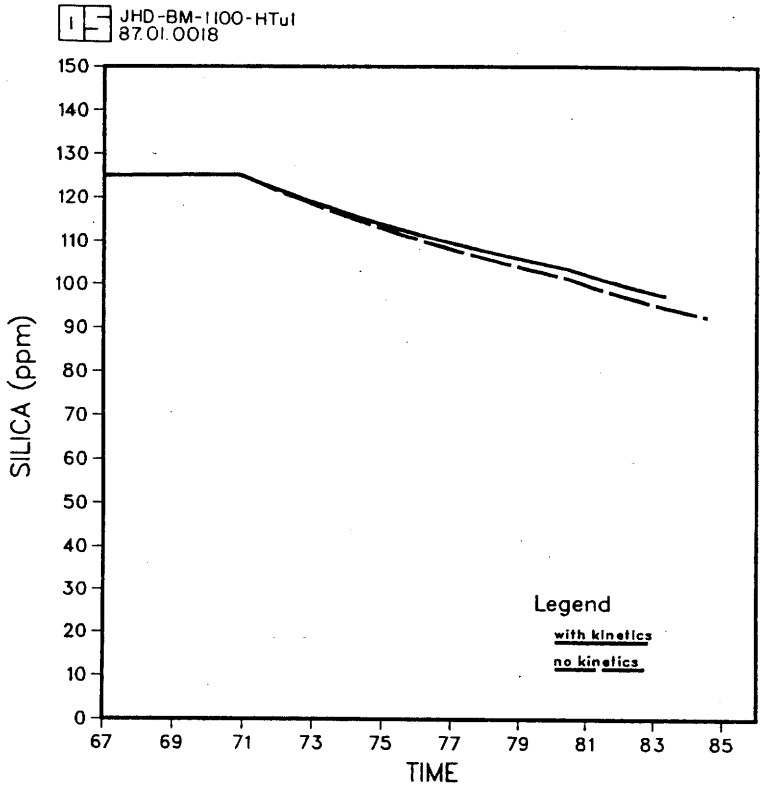

FIGURE 31 Silica versus Time without Kinetic Transport Using the "Best" Simple Model

Table 6 lists the concentrations used for each fluid type for the four chemical components modeled. Since the results of the matches described above performed on the Seltjarnarnes geothermal field were in close agreement, the chemistry match in this study was not aimed towards verifying field parameters such as the permeabilities, porosities, and reservoir volume. Rather, the purpose of the study was to estimate the boundaries of the seawater adjacent to the wellfield.

The results of the chemistry match are plotted for each well and for each chemical component: chloride, sodium, silica and oxygen-18, respectively, in Figures 32 through 35. For the best match, the seawater boundary follows approximately the land/sea boundary, surrounding the wells on three of four sides, and lying within 350 meters of wells SN-02 and SN-05 to the northeast. Figure 36 shows the suggested seawater/meteoric water boundary. The cross-hatched region contains the meteoric water; the area outside this region contains seawater.

TABLE 6. Values for the concentrations of the chemical species for the different fluids used in modeling the Seltjarnarnes geothermal field (oxygen-18 in per mill, deviation from standard ocean water, all other components in ppm).

Component	Seawater	Meteoric Water
Chloride	19,000	500
Sodium	10,500	300
Oxygen-18	0.001	-10.5
	5	130.0 (at 110°C)
Silica		
	5	80.0 (at 75°C)

The results also raised several questions. The matches with the oxygen-18 data for the individual wells were not good; the numerical model showed a much more rapid increase in oxygen-18 than the field data does. The same valve of 25.0 m^{-1} for A/V as for the silica was used for the kinetic reaction for oxygen-18. The results indicate that the exchange reactions of the oxygen isotopes are much slower than assumed for this model and that 25 m^{-1} is too high a value for A/V. The poor match for oxygen-18 could also inply that a three-dimensional model of the system is necessary, with fluid of a third chemical composition, of meteoric origin and containing less (< -10.5 per mil) oxygen-18, entering the system. The review by Hettling (1984) of other geothermal systems close to the Seltjarnarnes geothermal field suggest that a third type of fluid with a lower oxygen-18 content recharges these systems at depth from an inland source, while seawater intrudes into the fields at the shallower depths.

The match with the sodium data was not very good when a simple, dilution model was used. This is due to the fact that unlike the concentration of chloride, that of sodium is controlled by temperature dependent equilibria with various minerals. Those equilibria are mostly simple ion exchange reactions with calcium and hydrogen ions, and are known to occur rapidly.

There is considerable scatter in the measured silica concentrations from the wells. In samples taken before 1981 the scatter could possibly be due to improper sampling (no dilution) and analytical deviation, but not in the samples collected since 1981. Both the temperature of the water and the silica concentration vary with the production rate. Even allowing for these factors, a distinct trend of silica decrease is observed.

It is generally accepted that geothermal waters in Iceland equilibrate metastably with chalcedony, rather than with quartz, at temperatures below approximately 180°C (see Arnórsson et al. 1983). This is the basis of a geothermometer widely used in Iceland. When production from the Seltjarnarnes field began, the measured temperature and the calculated chalcedony temperature were in reasonable agreement, indicating that the fluids were probably in equilibrium with chalcedony. The insignificant temperature decrease measured since then and the downward trend in silica concentration (chalcedony temperature) together suggest that the Seltjarnarnes fluids are no longer in equilibrium with chalcedony and that kinetics do indeed play a role in the chemistry of the field.

To achieve the best match for silica, the A/V value was set at 25.0 m^{-1}. The value of 25.0 for A/V m^{-1} indicates moderately rapid kinetic reactions. The silica match would probably improve if a three-dimensional model with a third type of fluid of meteoric origin were used as suggested by the oxygen-18 modeling. The three-dimensional model might also show the role of the kinetic transport to be less significant, in agreement with the earlier results.

Although the chemistry modeling has identified some shortcomings of the two-dimensional model, the model can be used to predict roughly the future influence of the seawater on the system. Thus, an estimate of the amount of influx of seawater into the field over the next fifteen or twenty years could be obtained. From this information, the potential corrosion problems in the future may be identified and the necessary steps taken to minimize or alleviate these problems.

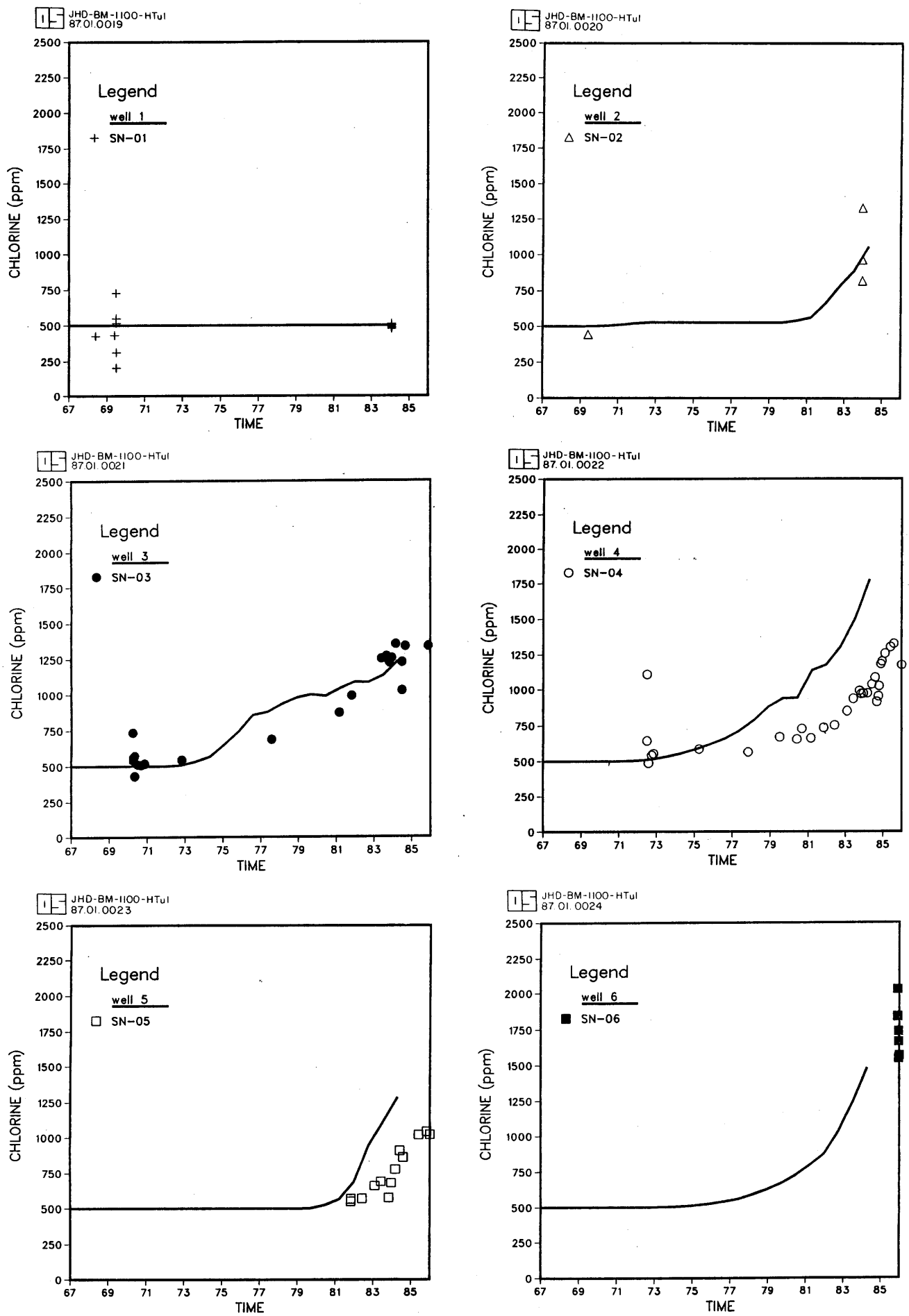

FIGURE 32 Chloride versus Time Showing the Match between the Numerical Model and Data for Individual Wells

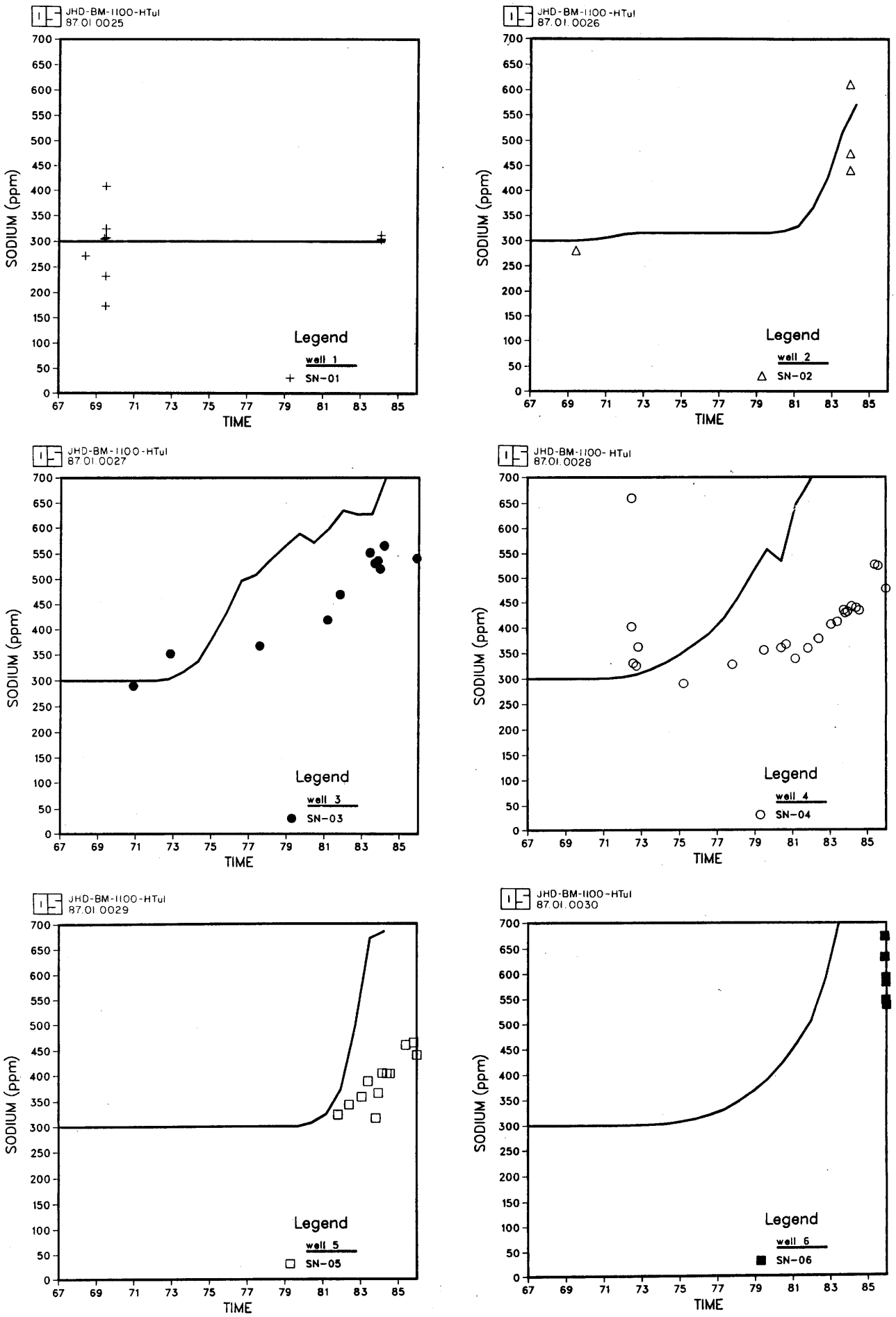

FIGURE 33 Sodium versus Time Showing the Match between the Numerical Model and Data for Individual Wells

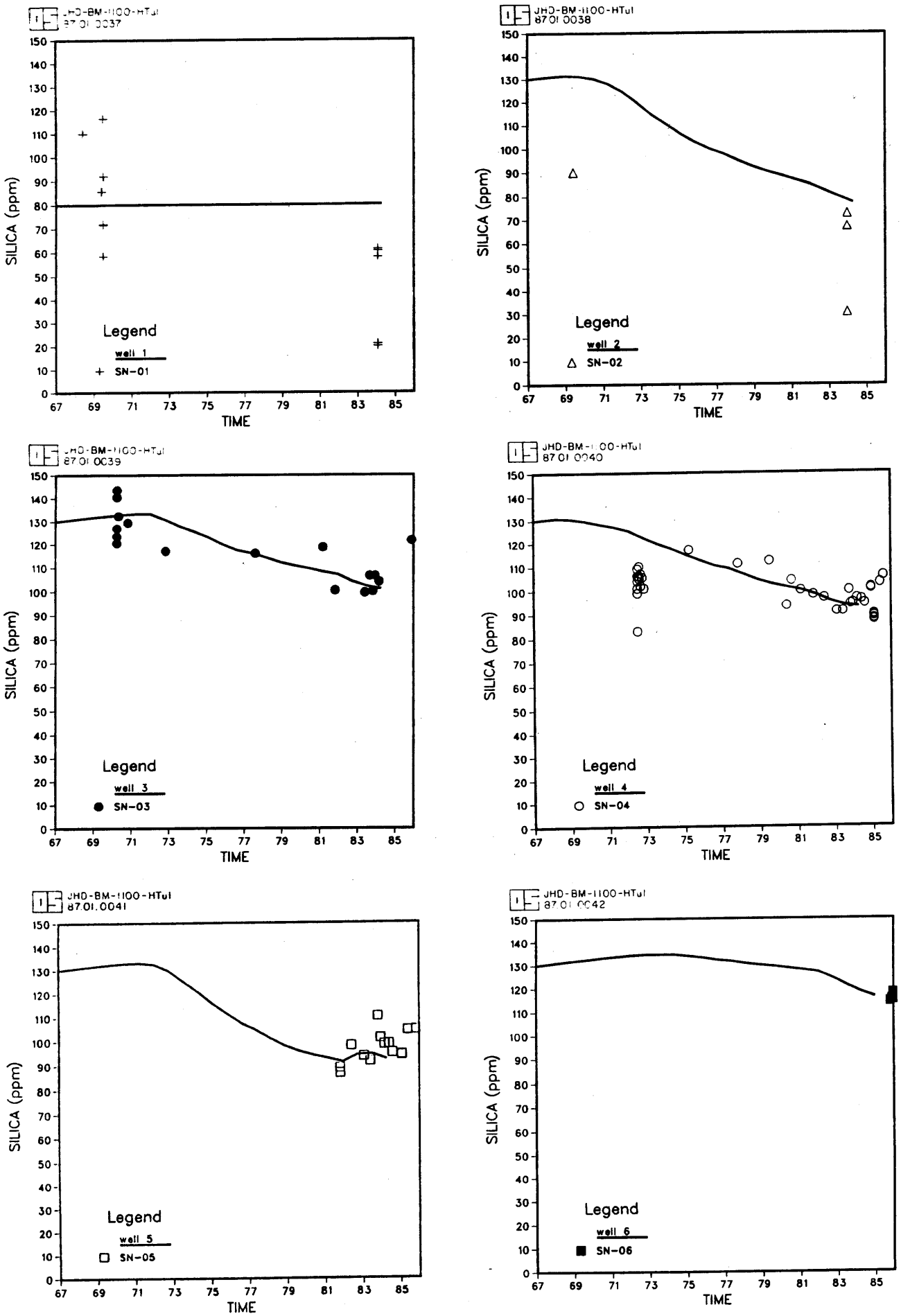

FIGURE 34 Silica versus Time Showing the Match between the Numerical Model and Data for Individual Wells

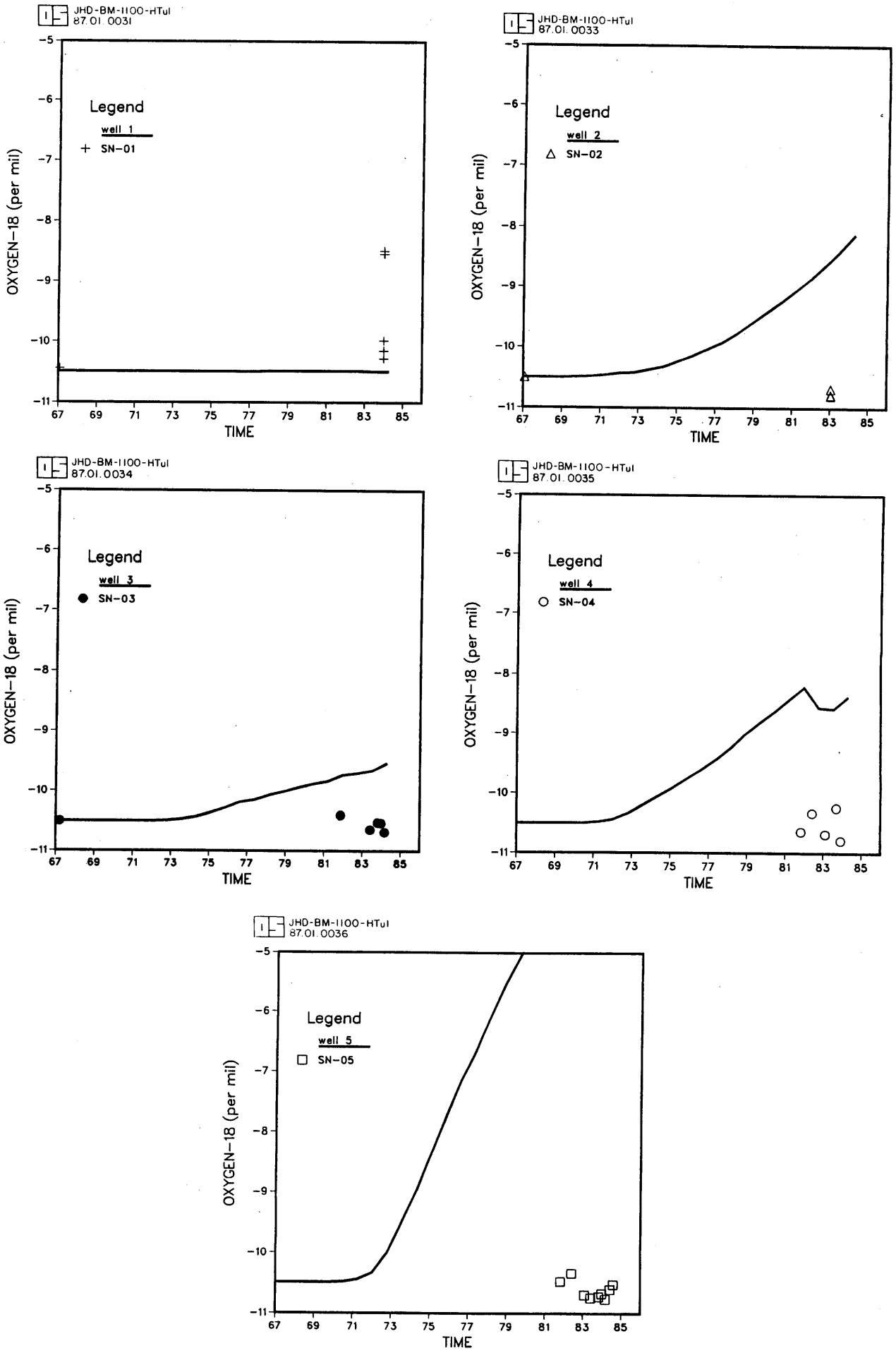

FIGURE 35 Oxygen-18 versus Time Showing the Match between the Numerical Model and Data for Individual Wells

5 PERFORMANCE PREDICTIONS

The main objective of this reservoir simulation study was to construct a model of the geothermal reservoir and use that model to predict changes in pressure, temperature and chemical composition with future production. The model that gave the best match with the production history was used to predict the changes for the next 20 years.

Three cases were studied:

a) Average yearly production of 70 l/s.
b) Average yearly production of 70 l/s for the first five years, then 12 l/s increase in production every five years from a new well close to well SN-03.
c) Average yearly production of 70 l/s for the first five years, then 30 l/s increase in production every five subsequent years from two new wells close to well SN-05.

Figures 37 a, b and c show the calculated drawdown in well SN-02 and the average drawdown for those three cases after 20 years and the measured drawdown in the same well. For the simulation a production history from August 1966 to October 1984 was used. When the data had been matched using trial and error, simulation data from October 1984 until September 1986 was added to the production history. As can be seen in Figure 31 the new data indicate more pressure drawdown for the last two years in the field than was calculated using the earlier match.

The reason for this difference could be effects of the size of the reservoir, or that the match using the data until 1984 is a little to conservative. It should also be kept in mind that all the production data is estimated. The performance predictions are therefore not very reliable and probably rather conservative, both for pressure and temperature.

The match with the changes in the chemical composition was not good (Chapter 4.5) because of three-dimensional effect. No future prediction was done for the chemistry because of this. It is apparent though that the salinity will continue to increase with the same slope as before, and if the production is increased the rate of increase will be accelerated.

The pressure drawdown after 20 years with no increase in production (case (a)) is estimated to be 7.4 bars in wells SN-04, SN-05 and SN-06, and the temperature decrease to be 3°C in well SN-04 and less in the others.

For case (b) the average pressure drawdown after 20 years was calculated to be 10.7 bars in well SN-06 and the temperature decline about 6°C in well SN-04. The average pressure drawdown for case c was calculated to be 15.5 bars in well SN-06 and 7°C decline in temperature in well SN-04.

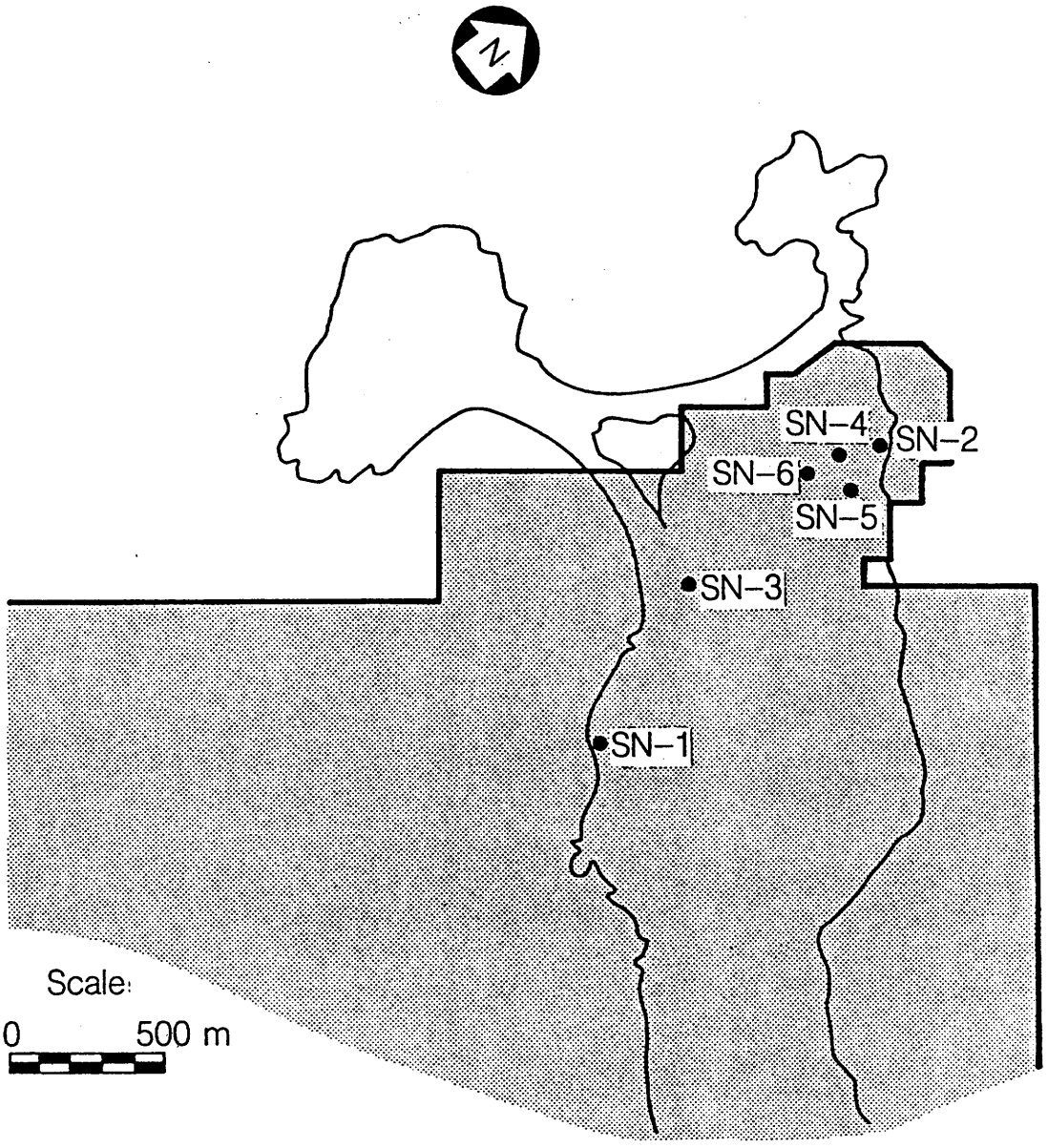

XBL 8612-12846

FIGURE 36 Suggested Boundary Between Seawater and Meteoric Water

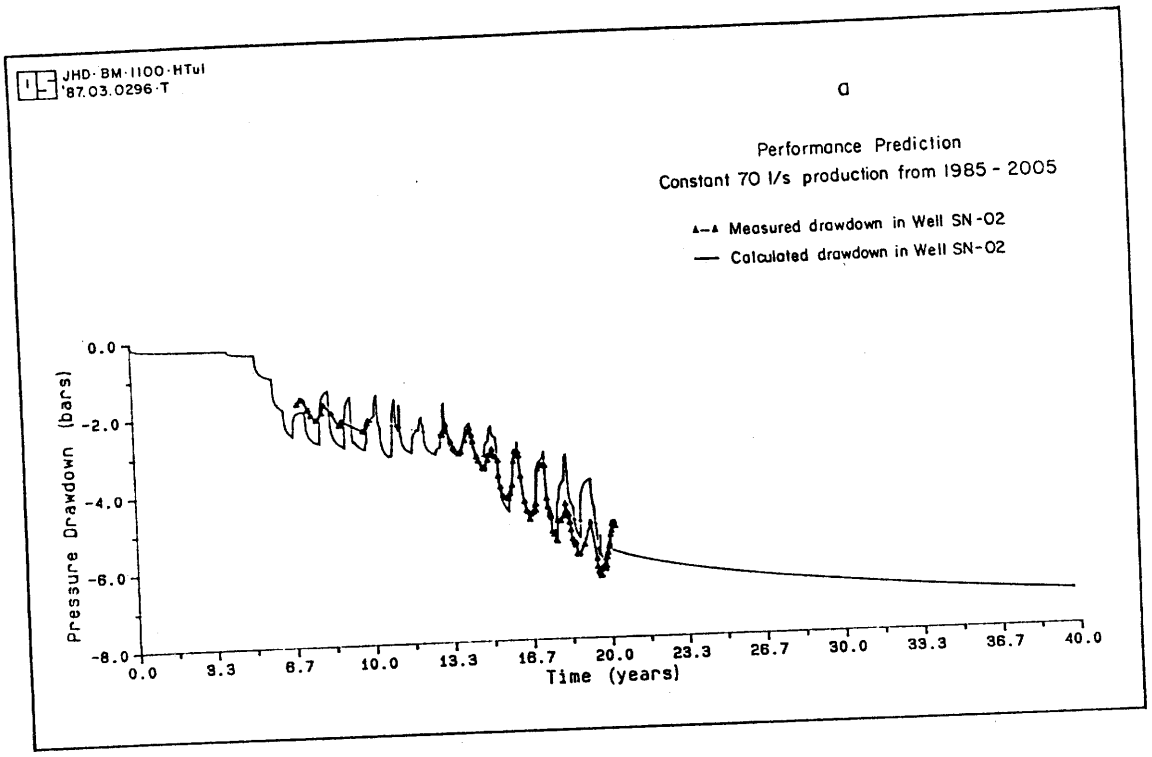

FIGURE 37 Pressure Performance Predictions

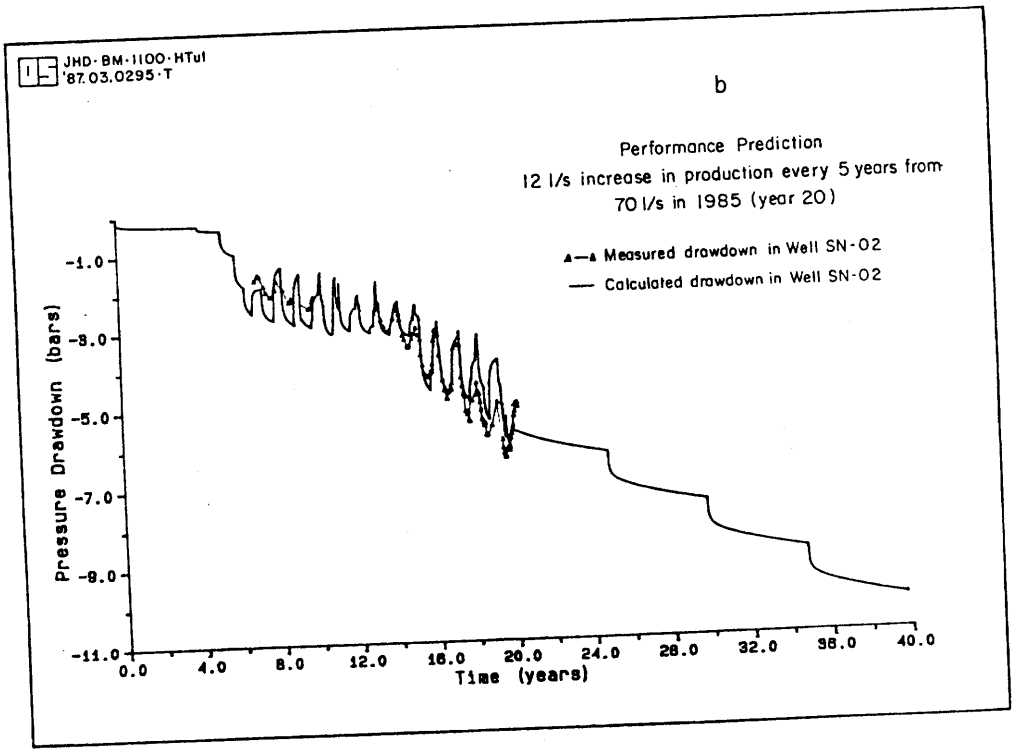

FIGURE 37 Cont.

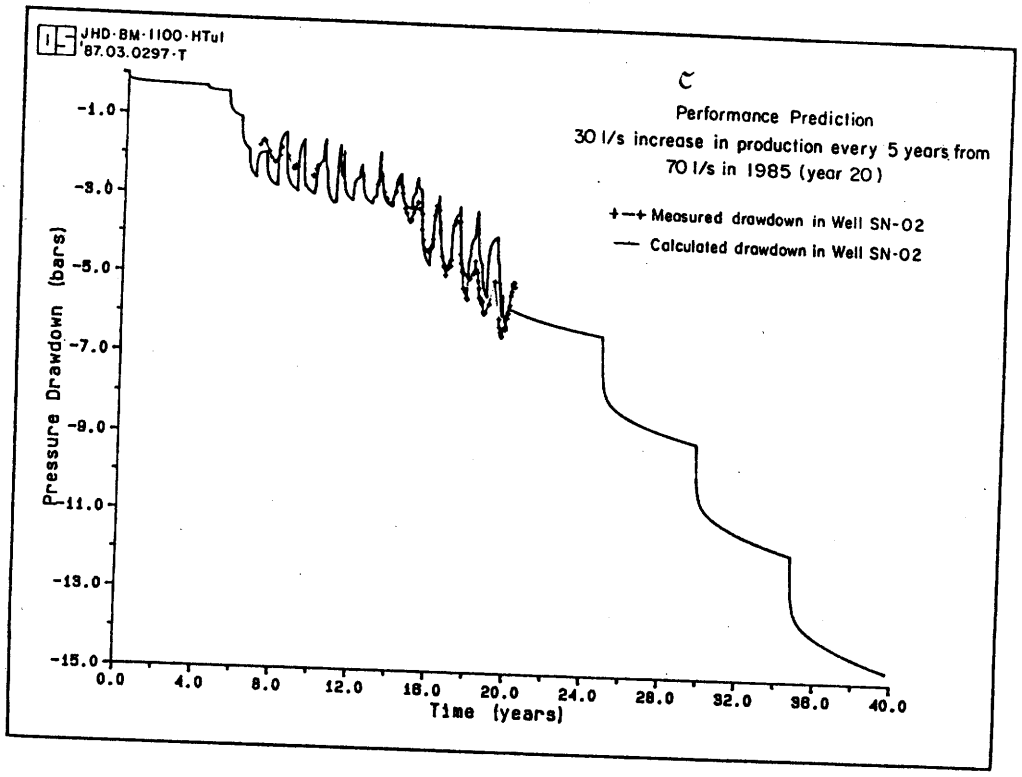

FIGURE 37 Cont.

6 CONCLUSIONS

A two-dimensional model of the Seltjarnarnes geothermal field in Iceland has been developed, incorporating thermal, chemical and pressure transient data. The model used to match the observed drawdown data has six regions of different permeabilities and porosities. The wellfield lies within a region of high permeability (80 md) and low porosity (2%). In the models the porosities increase away from the field, up to 15% at a distance of 4 km. The model shows no thermal decline, in agreement with observed data. The fluid chemistry modeling indicates that the seawater is very near the wellfield to the northwest. The performance predictions indicate an average drawdown of 15.5 bars over 20 years and a maximum temperature decline of 9°C, if the production of the field were to increase by 30 l/s every five years beginning in 1991. From the pattern of the observed chemical data, the salinity could increase greatly under this production scheme. To get a better predictions for the increase in salinity with further production it is necessary to continue this work and add the third dimension. Obtaining a better match with the pressure changes for the last two years would also improve the accuracy of the performance predictions.

7 ACKNOWLEDGEMENTS

The primary author would like to thank the National Energy Authority of Iceland for sponsoring her work at LBL, and the Earth Sciences Division of LBL for their cooperation during this work. The authors thank the Seltjarnarnes District Heating Service for allowing publication of the field data. This work was supported by the National Energy Authority of Iceland and the U.S. Department of Energy through Contract No. DEAC03-76SF00098 by the Assistant Secretary for Conservation and Renewable Energy, Office of Renewable Technology, Division of Geothermal Technology.

REFERENCES

Árný E. Sveinbjörnsdóttir, Jens Tómasson, Þorsteinn Thorsteinsson, 1984a: Seltjarnarnes, hola SN-05. Framkvæmd borunar, jarðlagaskipan og örvunaraðgerðir. Orkustofnun, Report OS-84091/JHD-41 B.

Árný E. Sveinbjörnsdóttir, Dagbjartur Sigursteinsson, Helga Tulinius, Hrefna Kristmannsdóttir, Sigurður Benediktsson, 1984b: Seltjarnarnes hola SN-06. Borun fyrir 13 3/8" fóðringu i 416 m. Orkustofnun, Report OS-84081/JHD-34 B.

Árný E. Sveinbjörnsdóttir, 1986: Seltjarnarnes hola SN-06, borun vinnsluhluta holunnar. OS-in print.

Bragi Árnason, 1976: Groundwater Systems in Iceland Traced by Deuterium. Soc. Sci. Isl. v. XLII, 236 pp.

Craig, H., 1961: Isotopic Variations in Meteoric Waters. Science, Vol. 133, pp 1702-1703.

Duff, I.S., 1978: MA28-A Set of Fortran Subroutines for Sparse Unsymmetric Linear Equations. Harwell Report AERE-R 8730, Oxfordshire, UK.

Edwards, A.L., 1970: TRUMP: A Computer Program for Transient and Steady-State Temperature Distribution in Multidimensional Systems. Lawrence Livermore Laboratory Report UCRL-14754, Rev 4.

Guðmundur S. Böðvarsson, 1981: Mathematical Modeling of the Behavior of Geothermal Systems Under Exploitation. Ph.D. dissertation, University of California, Berkeley.

Guðmundur Pálmason, Valgarður Stefánsson, Sverrir Þórhallsson, Þorsteinn Thorsteinsson, 1983: Geothermal Field Developments in Iceland. Ninth Workshop on Geothermal Reservoir Engineering, Stanford, Cal.

Helga Tulinius, Ómar B. Smárasson, Jens Tómasson, Ingvar B. Friðleifsson, Guðlaugur Hermannsson, 1986. Hitastigulsboranir árið 1984 á höfuðborgarsvæðinu, holur HS-14 til HS-22. Orkustofnun, Report OS-86060/JHD-22 B.

Hettling H.K., 1984: The Chemical and Isotopic Changes in the Low-Temperature Areas at Laugarnes, Elliðaár and Reykir: UNU Geothermal Training Programme, Iceland, Report 1984-3.

Hrefna Kristmannsdóttir, 1983: Breytingar a efnasamsetningu jarðhitavatns á Seltjarnarnesi á tímabilinu 1970-1983. Orkustofnun, Report OS-83106/JHD-19.

Hrefna Kristmannsdóttir, 1984a: Niðurstöður efnagreininga á djúpsýnum úr borholum SN-1 og SN-2 a Seltjarnarnesi. Orkustofnun, Report OS-84068/JHD-27 B.

Hrefna Kristmannsdóttir, 1984b: Rannsóknir fyrir Hitaveitu Seltjarnarness, 1984. In-house report, Orkustofnun, Iceland, HK-84/02.

Hrefna Kristmannsdóttir, 1984c: Aðgerðir í SN-4 í ágúst 1984. In-house report, Orkustofnun, Iceland, HK-22.08.1984.

Hrefna Kristmannsdóttir, 1986: Exploitation-Induced Infiltration of Seawater into the Seltjarnarnes Geothermal Field, Iceland. Geothermal Resources Council Transactions, v 10, pp. 389-393.

Hrefna Kristmannsdóttir, Helga Tulinius, 1984: Frumniðurstöður mælinga og efnagreininga á djúpsýnum úr holu SN-4 á Seltjarnarnesi. In-house Report, Orkustofnun, Iceland, H.K.-H.Tul/8406.

Hrefna Kristmannsdóttir, Þorsteinn Thorsteinsson, Jens Tómasson, 1984: Varðar rannsóknir og borun fyrir hitaveitu Seltjarnarness. In-house Report, Orkustofnun, Iceland, 84.02.10.

Jens Tómasson, Kristján Sæmundsson, 1970: Efnagreiningar á vatni úr holu S-3, á Seltjarnarnesi. In-house Report, Orkustofnun, Iceland, November.

Jens Tómasson, Þorsteinn Thorsteinsson, Hrefna Kristmannsdóttir, Ingvar Birgir Friðleifsson, 1977: Höfuðborgarsvæði, Jarðhitarannsóknir 1965-1973. Orkustofnun, Report, OSJHD-7703. Prepared for Hitaveita Reykjavíkur.

Lai C.H. 1985: Mathematical Models of Thermal and Chemical Transport in Geologic Media. Ph.D. Thesis, University of California, Berkeley.

Lúðvík Georgsson, 1985: Höfuðborgarsvædi-Borgarfjörður, niðurstöður viðnámsmælinga. Orkustofnun, Report OS-85111/JHD-14, pp.

Ómar Sigurðsson, Snorri P. Kjaran, Þorsteinn Thorsteinsson, Valgarður Stefánsson, Guðmundur Pálmason, 1985: Experience of Exploring Icelandic Geothermal Reservoirs. GRC 1985 International Symposium on Geothermal Energy, Kailua-Kona, Hawaii, Aug. 26-30.

Spencer, A., 1986: Development of a Method to Predict the Temperature Decline in Low Temperature Geothermal Systems under Exploitation Utilizing Temperature, Pressure and Chemical Transport Data. Masters Thesis, University of California, Berkeley.

Stefán Arnórsson, Einar Gunnlaugsson and Hörður Svavarsson, 1983: The chemistry of geothermal waters in Iceland. III. Chemical geothermometry in geothermal investigations. Geochim. Cosmochim. Acta 47: 567-577.

Svanbjörg H. Haraldsdóttir, 1984a: Seltjarnarnes hola SN-1, borholumaelingar. Orkustofnun, Report OS-84059/JHD-19 B, pp.

Svanbjörg H. Haraldsdóttir, 1984b: Seltjarnarnes hola SN-2, borholumaelingar. Orkustofnun, Report OS-84059/JHD-20 B, pp.

Svanbjörg H. Haraldsdóttir, 1984c: Seltjarnarnes hola SN-5, hitamaelingar. Orkustofnun, Report OS-84059/JHD-21 B, pp.

Þorsteinn Thorsteinsson, 1970a: Varðar holu 3 á Seltjarnarnesi. In-house Report, Orkustofnun, Iceland, ÞTH. 18.08.1970.

Þorsteinn Thorsteinsson, 1970b: Vatnsvinnsla og vatnsstöðumælingar i borholum á Seltjarnarnesi í ágúst-sept 1970. Draft at Orkustofnun, Iceland.

Þorsteinn Thorsteinsson, 1980: Staðsetning holu S-5 á Seltjarnarnesi. In-house Report, Orkustofnun, Iceland, ÞTH.-80104

Þorsteinn Thorsteinsson, 1985. Örvun og afkastageta holu SN-6 á Seltjarnarnesi. In-house Report, Orkustofnun, Iceland, ÞTH-85/06.

Þorsteinn Thorsteinsson, Jónas Elíasson, 1970: Geohydrology of the Laugarnes hydrothermal systems in Reykjavik. Geothermics, v. 2, Special Issue, p.1191.

Þorsteinn Thorsteinsson, Jens Tómasson, 1972. Vatnsvinnsla úr holu S-4 á Seltjarnarnesi. In-house Report, Orkustofnun, ÞTh./J.T. 30.8.72.

Þorsteinn Thorsteinsson, Hrefna Kristmannsdóttir, Árný E. Sveinbjörnsdóttir, Helga Tulinius, 1985: Áætlun um loftdælingar og pökkun í holu SNJ-6 á Seltjarnarnesi. In-house Report, Orkustofnun ÞTh-HK-AES-HTul-85/02.